MACHINE LEARNING & DATA ANALYTICS

FRIEDRICH-ALEXANDER UNIVERSITÄT ERLANGEN-NÜRNBERG
TECHNISCHE FAKULTÄT

Heart Rate Variability Analysis for Unsupervised Tilt Table Testing during Daily-life Activities

Bachelor's Thesis in Medical Engineering

submitted
by

Daniel Krauß

born 02.10.1996 in Schwäbisch Hall

Written at

Machine Learning and Data Analytics Lab (CS 14)
Department of Computer Science
Friedrich-Alexander-Universität Erlangen-Nürnberg (FAU)

Advisors: Robert Richer M.Sc., Martin Ullrich M.Sc., Prof. Dr. med. Jochen Klucken, Prof. Dr. Bjoern Eskofier

Started: 01.09.2018

Finished: 31.01.2019

Ich versichere, dass ich die Arbeit ohne fremde Hilfe und ohne Benutzung anderer als der angegebenen Quellen angefertigt habe und dass die Arbeit in gleicher oder ähnlicher Form noch keiner anderen Prüfungsbehörde vorgelegen hat und von dieser als Teil einer Prüfungsleistung angenommen wurde. Alle Ausführungen, die wörtlich oder sinngemäß übernommen wurden, sind als solche gekennzeichnet.

Die Richtlinien des Lehrstuhls für Bachelor- und Masterarbeiten habe ich gelesen und anerkannt, insbesondere die Regelung des Nutzungsrechts.

Erlangen, den 31st January 2019

Übersicht

Eine Auswirkung des demographischen Wandel ist, eine höhere Lebenserwartung. Das bringt eine Reihe neuer medizinischer Herausforderungen mit sich, wie die Behandlung von neurodegenerativen Krankheiten. Diese Erkrankungen können die Funktionalität des Autonomen Nervensystems beeinflussen, was zu einer Minderung der Herzrate und einer schwächeren Orthostasereaktion führt. Aufgrund der hohen Zahl an Patienten und der Notwendigkeit von längerfristigen Untersuchungen wird eine eigenständige Datenaufnahme immer wichtiger. Das Ziel dieser Bachelorarbeit war die Entwicklung eines Systems, welches eine unbeaufsichtigte Analyse von Herzratenvariabilität nach Lagewechseln möglich macht. Dafür wurden zwei Algorithmen entwickelt: Der erste zur Lagebestimmung, der zweite zur Analyse der Herzratenvariabilität. Zur Bestimmung der aktuellen Lage wurden zwei IMU Sensoren verwendet: Der erste Sensor, welcher an der Brust platziert wurde, war mit einem Beschleunigungssensor, einem Gyroskop und einem Barometer ausgestattet. Als zweiter Sensor, welcher am Bein platziert war, wurde der interne Beschleunigungssensor eines Smartphones verwendet. Durch die Berechnung des Winkels zwischen den jeweiligen Beschleunigungsvektoren konnte zwischen sitzen, liegen und stehen unterschieden werden. Anstrengende Aktivitäten wie Rennen oder Treppensteigen sollten nicht berücksichtigt werden. Dafür wurde ein „static angle detector“ sowie das Barometer verwendet. Eine Studie, welche Situationen aus dem täglichen Leben simuliert, wurde durchgeführt um das System zu evaluieren (N=10). Dazu wurde die resultierende Lage in jeden Datenpunkt analysiert. Durch die Nichtberücksichtigung von Datenpunkten zwischen zwei unterschiedlichen Lagen wurde eine Treffergenauigkeit von 92.93 % erreicht. Dabei wurde Liegen zu 100 % erkannt. Die Erkennung von Lagewechseln war in 81.14 % der Fälle erfolgreich. Aufgrund der Vielzahl an Lagewechseln pro Tag ist es jedoch nicht nötig dass alle Lagewechsel erkannt werden.

Zur Analyse der Herzratenvariabilität wurden mehrere zeit- und frequenzbasierte Ansätze implementiert. Zur Beurteilung des Algorithmus wurde eine Studie mit einem Lagewechsel durchgeführt (N=10). Dabei war in allen Messwerten eine klare Veränderung ersichtlich. Dabei muss aber berücksichtigt werden, dass der frequenzbasierte Ansatz eine mehr als 15 mal so große Veränderung gezeigt hat. Jedoch war auch die Standardabweichung von 1203 % sehr groß. Mögliche Gründe für die hohe Standardabweichung sind die mit nur einer Minute zu kurzen Zeitintervalle. Zukünftige Forschungen sollten zeit- und frequenzbasierte methoden kombinieren um sowohl die kurzfristige als auch die langfristige Funktionalität des Autonomen Nervensystems zu bewerten.

Beide Auswertungen haben gezeigt, dass es möglich ist ein System zu entwickeln, welches eine unbeaufsichtigte Bewertung der Orthostasereaktion nach Lagewechseln möglich macht.

Abstract

Triggered by the demographic change, people live longer. That brings forth new medical challenges like the treatment of neurodegenerative diseases. These illnesses could affect the functionality of the autonomic nervous system. That leads to a depressed heart rate variability and a lowered orthostatic reaction. Due to the huge amount of patients and the requirement of long-term recordings, the possibility of unsupervised home monitoring gets more important. The aim of this work was to develop a system for unsupervised heart rate variability analysis after posture changes. Therefore, two algorithms were developed: One to detect posture changes and one to evaluate the change in heart rate variability. To determine the actual posture, two IUM sensor units were used. The first sensor was integrated in a chest worn strap, containing accelerometer, gyroscope and barometer. As leg sensor, the internal accelerometer of an Android smartphone was utilized. Sitting, lying and standing could be distinguished by computing the angle between the acceleration vectors of the devices. To reject exhausting activities like running or stair climbing, a static angle detector and a barometer were used. As evaluation, the system was tested in a user study which simulated daily life activities (N=10). To assess the performance, the detected postures were analyzed sample by sample. After rejecting the samples happened during posture changes, a recognition rate over all postures of 92.93 % was achieved. Thereby, the detection of lying reached an accuracy of 100 %. For the detection of posture changes, a recognition rate of 81.14 % was achieved. Due to the big amount of postural transitions per day, it is not fatal that some posture changes were not detected.

To analyze the heart rate variability, several time- and frequency-based features were implemented. As evaluation a study, containing one postural transition, was conducted (N=10). Thereby all features indicated a clear change, whereas the change in the frequency-based approach was more than 15 times larger than the change in time-domain measures. Though, the frequency-based measure had a standard deviation of 1203 %. A reason of this might be the short recording time of only one minute per posture. Future investigations should combine long-term frequency based analysis with short-term time-based analysis.

Both evaluations proved, that it is possible to establish a home monitoring system to evaluate the orthostatic reaction after posture changes.

Contents

Chapter 1

Introduction

Over the last two hundred years quality of life has been increased steadily because of better hygiene, better patient care, and new medical treatment possibilities. This demographic transition was triggered off by an economic transition, better known as *industrial revolution*, which led to better education and economic growth. One general effect of this demographic change is increased life expectancy. [Cer17] This also leads to an increase in widespread diseases like cardiovascular diseases, cancer or neurodegenerative disorders. One of the most prominent examples of the latter group is ***Parkinson's Disease (Parkinson's)*** [Asc05].

Parkinson's is a widespread illness all around the world. About one percent of the world's population over the age of 65 suffers from ***Parkinson's*** [Bea15]. The most prominent and visible symptoms of ***Parkinson's*** are a decrease in motor capability like hand tremor, postural instability and freezing of gait [Asc05]. Moreover, it also affects the ***Autonomic Nervous System (ANS)***, which leads to disorders in cardiovascular regulation, particularly to orthostatic hypotension, sleep disturbance and sexual dysfunction [Asc05] [Mih06].

Under normal circumstances the ***ANS*** regulates heart rate in order to quickly adapt the cardiovascular system to situations like increased physical activity, stress exposure or postural changes (also known as ***Heart Rate Variability (HRV)***) [Lan07]. During posture changes, changes in heart rate are mostly performed to prevent dizziness and impairment of consciousness. Therefore, ***HRV*** analysis has been proven to be a reliable indicator for the assessment of the ***ANS***. For a correct diagnosis, it is of particular importance to combine the ***HRV*** analysis with contextual information about postures and posture changes, e.g. transitions between sitting, lying and standing. However, if a patient suffers from a neurodegenerative disease, the reaction of the ***ANS*** might be depressed and can hence lead to vertigo or even syncope [Haa01] [Ric16] [Lan07].

The actual gold standard procedure for the estimation and determination of such an orthostatic dysregulation is the clinical *Tilt Table Test*. Thereby, a patient lies down on a special tilt table that simulates several posture changes from lying to standing in a fixed sequence. Blood pressure and heart rate are measured during this procedure to evaluate the reactivity of the ***ANS*** [Lc01] [Ben96].

However, since the procedure is performed in a clinical (and hence alien and unknown) environment, the patient's physiology might be influenced by stress, pressure or agitation. This is also referred to as *white coat syndrome* [Owe99]. Therefore, the ***HRV*** analysis should be performed in a natural home environment using unobtrusive measurement techniques to lower the white coat syndrome influence. This should increase the quality and reliability of results. Furthermore, it enables long-term measurements during daily-life activities. This leads to larger data sets and hence probably to a better diagnosis of a potential ***ANS*** dysfunction and its degree of severity.

However, an unsupervised home monitoring setting also means that a lot of data, not usable for subsequent clinical analysis, is collected. Therefore, only relevant posture changes should be detected, whereas others need to be rejected. For that reason, the goal of this thesis is to develop a system based on the groundwork Richer et al. in order to replace the clinical tilt table test with a home monitoring capable system [Ric16]. To establish such a home monitoring system wearables, which can be integrated in the patient's daily life, should be utilized. In this work, a chest worn sensor with ***Inertial measurement unit (IMU)*** and ***Electrocardiogram (ECG)*** recording as well as inertial sensors from a smartphone worn in a trouser pocket were used.

Within this thesis, two algorithms were developed: One algorithm for detecting postures and the changes between them, the other for computing features for ***HRV*** analysis triggered by those posture changes.

The structure of this thesis is organized as follows: In Chapter 2, the relevant related work is presented. Chapter 3 describes the medical background of the orthostatic reaction and the underlying cardiovascular regulation. In Chapter 4, the methods for the algorithms developed in this thesis are presented. For the evaluation of both algorithms, two separated studies were conducted, which are described in Chapter 5: One study evaluates the ***HRV*** analysis during posture changes, the other study assesses the posture change detection. The results of both studies are presented in Chapter 6 and discussed in Chapter 7. Chapter 8 contains a conclusion of the whole work and provides an outlook on possible future research issues.

Chapter 2

Related Work

2.1 Posture Change Detection

During the past years, many researchers have worked on the detection of postural transitions. There are a lot of different approaches like from Najafi et al. who investigated the correlation between the characteristics of postural transitions and the risk of falling in elderly people. Therefore, a gyroscope, which was attached at the subject's chest, was utilized [Naj02]. Kangas et al. conducted a pilot study to determine acceleration thresholds for fall detection. The accelerometers were placed on waist, wrist and head. The goal was to investigate which placement is best to distinguish potentially dangerous falls from daily life activities. The developed system was ought to perform in a unsupervised home monitoring environment [Kan07].

If more than one sensor is involved in the detection of postural transitions, it might be necessary to align them to the body. Palermo et al. did a body-to-sensor alignment through functional calibration for gait analysis. They were able to remove effects of different sensor placements on different body segments [Pal14]. To the same issue, US patent *US20090312973A1* [A.1] was published, presenting a system which automatically calibrates a posture sensor by detecting a walking state or a posture change.

Many papers were published about the detection of postures and the transitions between them: Bidargaddi et al. developed a wavelet based algorithm to determine the duration of sit-to-stand and stand-to-sit transitions by using a three-axis accelerometer which was fixed around the waist. Their goal was to evaluate the condition of patients with chronic diseases. [Bid07].

Another paper by Zijlstra et al. compared sit-to-stand and stand-to-sit transition detections based on motion sensors or force plates. Therefore, a study with older adults and ***Parkinson's*** patients was conducted. In this work, it could be shown that both detection methods had a

high agreement, except for the stand-up duration of ***Parkinson's*** patients [Zij12]. Additionally, several patents were published for detecting postures and posture changes, such as the US patents *US7210240B2* [A.2], *US5865760A* [A.3] and *US20080281381A1* [A.4].

For the performance of a sit-to-stand transition there are some issues that need to be considered, such as the sitting position. For that reason, Janssen et al. examined the ability of subjects to do a sit-to-stand movement in dependency of chair height, the availability of armrests and the foot position. [Jan02]. Goodfrey et al. compared two concepts to detect stand-to-sit and sit-to-stand transitions and their duration with one single triaxial accelerometer. The first approach was an algorithm that processes sensor data with a scalar product and vertical velocity estimates. Therefore, the accelerometer was placed at the chest. The second approach was to place the acceleration sensor at the lower back and to develop an algorithm based on vector magnitude and discrete wavelet transformation. While both algorithms showed good results with an accuracy of more than 86 %, the first approach performed better in estimating transition duration. [God14].

The base of this bachelors's thesis is the work of Richer et al. The work combines real-time ***HRV*** analysis with the detection of stand-up events using internal smartphone sensors. From the gravity and the magnetic field sensors, an orientation vector was computed. For the detection of a stand-up event, the pitch axis orientation was required to vary between 60° and 90°. To reduce false detections as a result of other inadvertent movements, the algorithm was combined with the smartphone's step detection sensor. Only if at least one step was detected within ten seconds after a possible stand-up event, it was considered valid. With this system, a recognition rate of 90 % was reached. It was observed that standing up too fast or too slow as well as an incorrect placement of the mobile phone in the pocket could cause the algorithm to fail [Ric16].

2.2 HRV Analysis

The term „***HRV***“ can be described with a variety of different features that all attempt to „quantify“ the subject's heart rate variability. For that reason, a task force, established by the Board of the European Society of Cardiology, was charged to develop appropriate standards. The specific goals were, inter alia, to standardize nomenclature and measurement methods, as well as to develop definitions of terms. The task force divided the different methods into the following subgroups: [Sch99]

- Time-domain measurements
  - Statistical measures
  - Geometric measures

- Frequency-domain measurements
  - Short-time recordings
  - Long-term recordings (e.g. over entire 24h)

The standard procedure to measure the ***HRV*** parameters are the Schellong, or the Tilt Table Test [Win05] [Lc01] [Ben96]. Therefore, an ***ECG*** recording is necessary. To make ***ECG*** measurements as comfortable as possible, especially for home monitoring scenarios, several research groups presented solutions for ***ECG*** measurement without conductive contact [Ale07] [Kim05] [Lim06]. Another approach is to directly include textile electrodes in everyday clothing. [Pol07].

Several publications worked with at least one of these measurement approaches: Kobayashi et al. examined the influence of paced breathing on the reproducibility of ***HRV*** measures. Therefore, a spectral analysis was done [Kob09].

Aysin et al. compared several time-domain methods with a frequency based measure with and without a respiration analysis. The additional information from respiration analysis enabled isolating sympathetic and parasympathetic branches in ***HRV*** signals for a more accurate reflection of ***ANS*** reactions. In contrast, US patent *US7079888B2* presented a method for monitoring the autonomic nervous system using a non-stationary spectral analysis of heart rate in combination with respiratory activity [A.8].

Garcia et al. performed a spectral ***HRV*** analysis using Wavelet transformation instead of the commonly used ***Fast Fourier Transformation (FFT)***. The authors suggest that wavelet-based analysis might perform better than ***FFT***, especially for analyzing fast transient events in RR time series [Gar13].

Abnormal ***HRV*** can be a predictor of certain diseases. Kudaiberdieva et al. published a review about ***HRV*** as a predictor of sudden cardiac death with the conclusion that reduced ***HRV*** is a strong prognosis of mortality in myocardial infarction and heart failure [Kud07]. Myers et al. compared different measurement methods to examine which one is the most useful to predict sudden cardiac death. It turned out that power spectral analysis methods were the best indicators for categorizing patients according to the risk of sudden cardiac death [Mye86]. Persson et al. investigated the influence of ***HRV*** in patients with untreated epilepsy. As a result, no significant influence was detectable [Per07].

HRV analysis is a common indicator for the correct functionality of the ***ANS***. Therefore, several different systems were developed and patented, such as US patents *US20080082001A1* [A.5], *US20120108916A1* [A.6] or *US20090005696A1* [A.7].

Since ***Parkinson's*** is a neurodegenerative disease many research groups analyzed the influence of ***Parkinson's*** based on ***HRV*** parameters. Haapaniemie et al., as well as Kallio et al., examined different ***HRV*** parameters of ***Parkinson's*** patients [Kal00] [Haa01]. Haapaniemie et al. conducted a study where 24 h ***ECG*** recordings of patients were acquired. Frequency-based ***HRV*** measures revealed a strong correlation between ***Parkinson's*** and a dysfunction of the ***ANS***. In addition to that, a more advanced disease progression led to a stronger ***ANS*** dysfunction [Haa01]. In comparison to that, Mihci et al. were not able to find a correlation between disease severity and the ***HRV*** measurements. Nevertheless, a significantly lower ***HRV*** was detected in different time- and frequency-based methods [Mih06].

Richer et al. conducted a study to analyze the orthostatic reaction after posture changes with healthy subjects and ***Parkinson's*** patients. For this purpose, several time-based analysis methods were used to evaluate the orthostatic reaction. Results showed a clear difference between healthy subjects and ***Parkinson's*** patients for all measures [Ric16].

Chapter 3

Medical Background

3.1 ECG-Measurement

The ***ECG*** is a standard, non-invasive procedure for measuring the electrical activity of the heart. It is defined as the potential difference on the human skin between two electrodes[Lan07].

The sinus rhythm of the heart, which is the usual, regular heart beat rhythm, is established by the sinus node. It consists of pacemaking cells that create electrical signals for every beat, hence causing the heart muscle cells to depolarize and contract. The action potentials of the single heart cells add up to one electric dipol on the skin which can be measured as potential difference by two surface electrodes (also referred to as *Lead*) [Lan07].

For allowing standardized ***ECG*** measurements the electrodes need to be positioned in a prescribed way. Einthoven's triangle describes the placement of three electrodes attached on the limbs (LA – Left Arm, RA – Right Arm, LL – Left Leg), forming a virtual triangle of three leads (see Figure 3.1(a)) [Lan07]:

- Lead I (RA – LA)
- Lead II (RA – LL)
- Lead III (LA – LL)

In this thesis, two electrodes were placed on the chest according to Lead II of Einthoven's triangle. Additionally, a third electrode, as depicted in Figure 3.1(b), was used for the Driven Right Leg circuit, which is often added to prevent electromagnetic interference [Win83].

An example of one cardiac cycle, as recorded by the ***ECG***, is illustrated in Figure 3.2. As depicted, the visible parts of one cardiac cycle can be divided into the following phases: [Lan07] [Ric15].

- **P wave:** Arterial systole contraction pulse
  Duration: 60-80 ms

- **PQ segment:** Represents the time the wave travels from the atrioventricular (AV) node towards the ventricles
  Duration: 60-80 ms
- **QRS complex:** Representation of the ventricle depolarization. The R peak shows the contraction of the left ventricle
  Duration: 80-100 ms
- **ST segment:** Time the ventricular cells are depolarized
  Duration: 100-120 ms
- **T wave:** Repolarization and relaxation of the left ventricle
  Duration: 120-160 ms

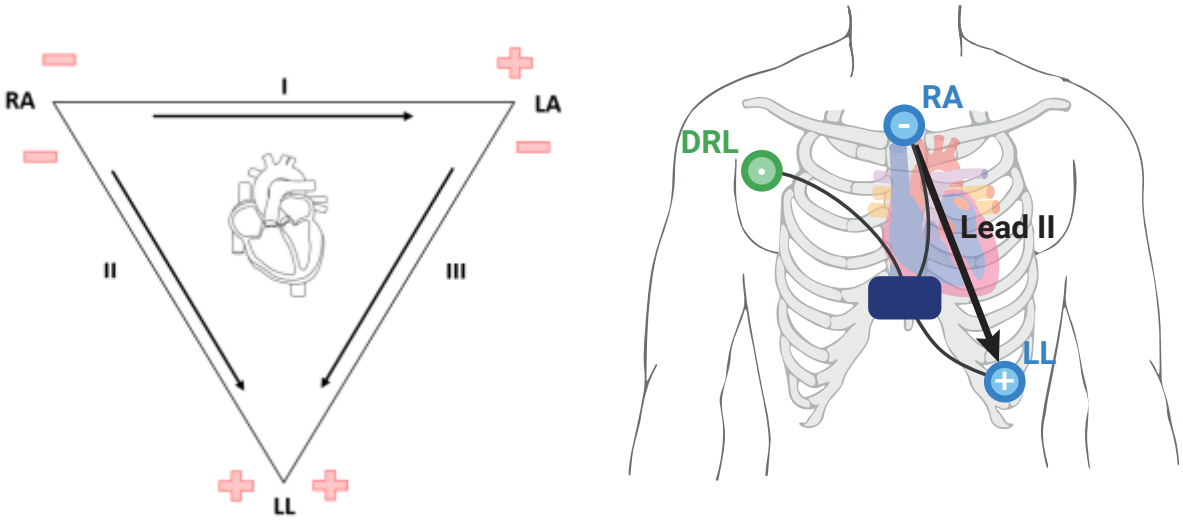

(a) Schematic representation of Einthoven's triangle [Wor]

(b) Lead II according to Einthoven's triangle [Ric15]

Figure 3.1: RA: Right Arm, **LA:** Left Arm, **LL:** Left Leg, **DRL:** Driven Right Leg

3.2 Circulatory System

Basically, the human's heart consists of two separated parts with one atrium and ventricle each. The right part of the heart pumps blood with low oxygen to the lungs, while the left part provides blood containing a high oxygen level.

The circulatory system of a healthy body usually contains a blood volume of about 5-6 liters. It mainly consists of the systemic circulatory system, which transports oxygenated blood away

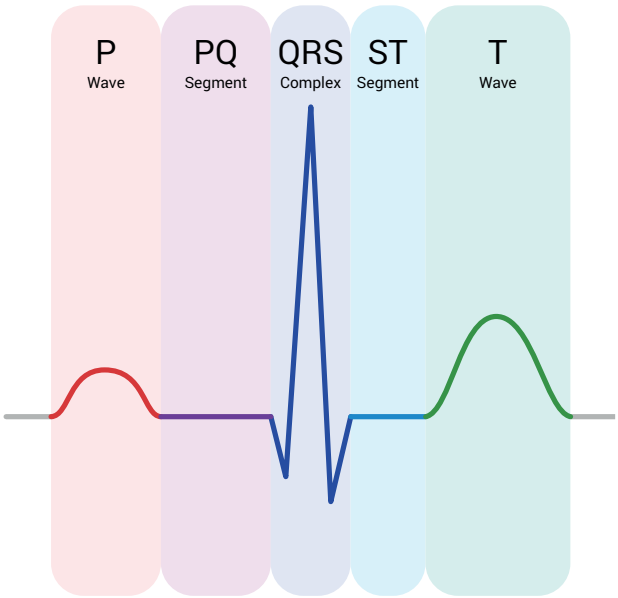

Figure 3.2: Schematic diagram of a normal sinus rhythm for a human heart as seen on ECG [Ric15]

from the heart and returns oxygen-less blood back to the heart. A schematic overview is shown in Figure 3.3.

The systemic circulation system also consists of two parts: The high and the low pressure system. The low pressure system is mainly composed of veins. Since their compliance is 200 times bigger, compared to the compliance of arteries, the low pressure system usually contains about 85% of the total blood volume. [Lan07]

The first transition point between both systems is the left side of the heart. During systole the heart pumps the blood from the left atrium (low pressure system) over the ventricle into the aorta which belongs to the high pressure system. The aorta has an elastic wall that helps to maintain a constant blood flow through the whole body. From there, blood is distributed to all organs through arteries and arterioles. The other transition point between high and low pressure system are the capillaries, which consist of lots of very small blood vessels. They are responsible for transferring blood into the venous system and for oxygen and nutrient exchange. Because of the high number of capillaries they have a small flow velocity which leads to longer contact time with the blood and better mass exchange [Lan07].

In order to close the circuit, the low oxygen blood has to be pumped back from the organs to the right heart chamber. However, blood pressure in the lower limbs is not big enough for the blood to flow back into the heart chambers autonomously (relative to hydrostatic pressure). Therefore, venous valves stop blood backflow into the lower extremities. Additionally, leg muscles

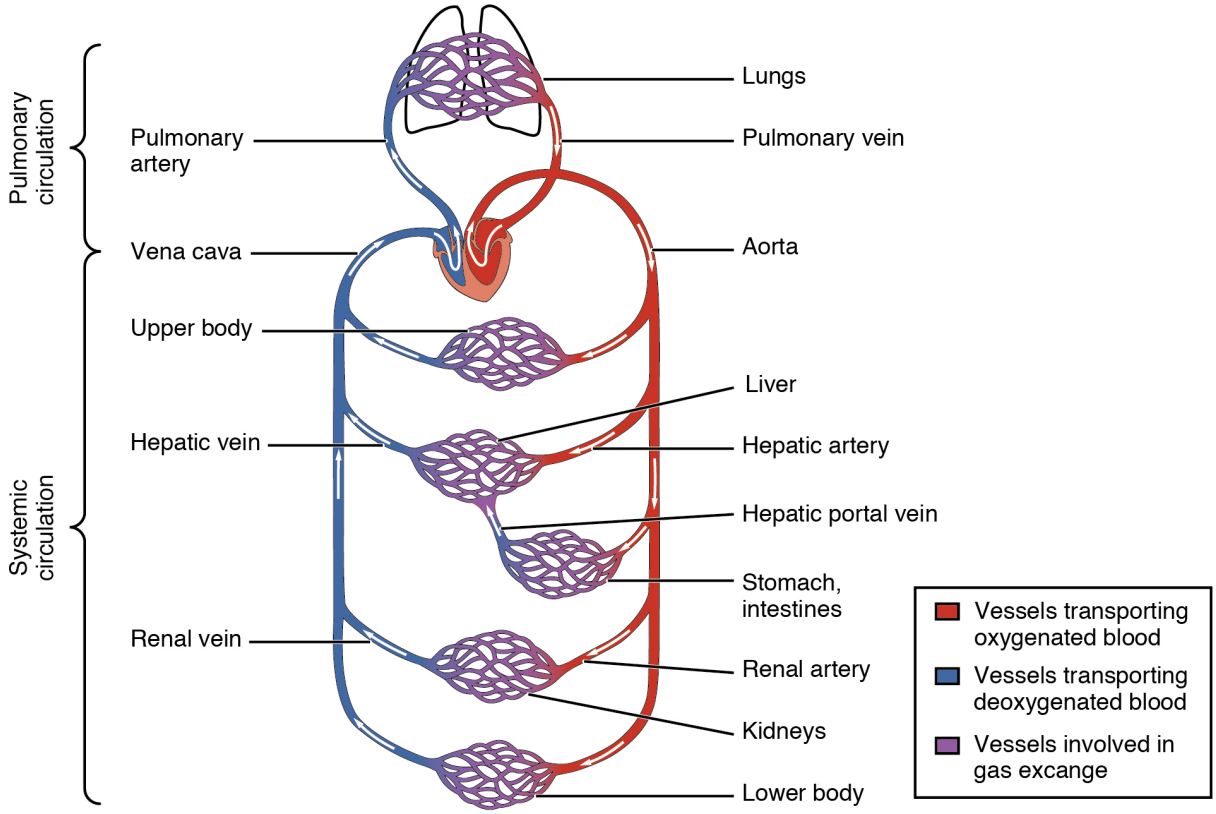

Figure 3.3: Circulatory system [Ope13]

help to press the blood back to the heart. From the right heart chamber the blood is transferred to the lungs to enrich it with oxygen for the systemic circulatory [Lan07].

Because of several parameters like blood volume, circadian rhythm, posture, outside temperature and activity, the blood pressure in the high pressure system varies in a certain range [Lan07]. Blood pressure values between 120/80 and 140/90 mmHg (systolic/diastolic) are considered as normal even it has to be mentioned that the normal blood pressure increases with aging [Lan07]. To supply all organs with sufficient oxygen and nutrients and to prevent damage of arteries and capillaries, the blood pressure needs to be regulated in order to ensure it is in the right range. An interaction of the sympathetic and the parasympathetic nervous system (two parts of the ***ANS***) is responsible for adjusting the right blood pressure [Lan07]. If receptors of the circulatory system detect a short-term decrease in blood pressure, the sympathetic nervous system gets activated and at the same time, the parasympathetic nervous system gets inhibited. This leads to a chain of reactions like an increase of heart rate and a decrease in artery compliance. If the sympathetic nervous system is activated over longer periods of time, the total blood volume is increased by the ***ANS***, which enforces adding water and salt to the circulatory system [Lan07].

3.3 Orthostatic Reaction

Another big influence on blood pressure is gravity, especially during posture changes. After changing posture from lying or sitting to standing, blood sacks into the legs due to increased hydrostatic pressure [Lan07]. As consequence, an increasing blood pressure in the lower body parts as well as a lower blood pressure in the upper body parts can be observed. If there was no adequate reaction of the organism, the blood supply to the brain would collapse, potentially resulting in vertigo and syncope [Lan07]. The human body commonly reacts to such posture changes by activating the symapthetic nervous system and inhibiting the parasympathtic nervous system. This leads to lower artery compliance, lower blood flow through the kidneys, an increase of the heart rate and a release of several hormones such as thyroid hormones [Lan07]. This reaction of the ***ANS*** is known as the „orthostatic reaction“. A regular orthostatic reaction causes a heart rate increase of about 30% and, in parallel, a decrease in ***HRV***. The lower ***HRV*** is caused by the requisiteness of a higher heart rate in a short time [Lan07]. The orthostatic reaction can be classified into the following phases: the *initial response* (first 30 seconds), the *early phase of stabilization* (first 1-3 minutes upright) and the *prolonged orthostatic stress* ($>$ 5minutes) [Wie09].

Disorders of the ***ANS***, such as ***Parkinson's***, can lead to decreased ***HRV*** as well as to a lower orthostatic reaction. As visualized in Figure 3.4, which shows the differences in orthostatic reaction between a healthy subject and a patient suffering from ***Parkinson's***, the orthostatic reaction might even not be present at all [Ric16].

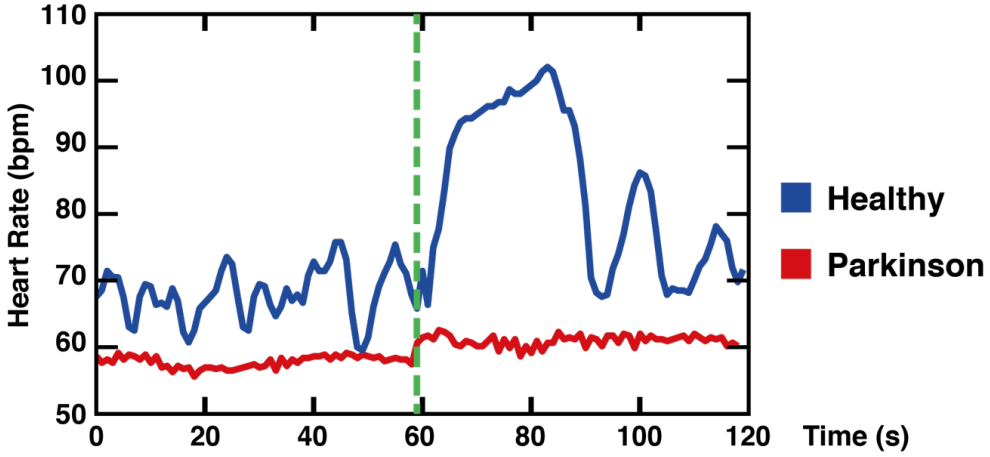

Figure 3.4: Orthostatic reaction of a healthy subject and a patient suffering from ***Parkinson's*** [Ric16]

There are two clinical procedures to evaluate the orthostatic reaction in the hospital: The Schellong and the Tilt Table Test. The Schellong test is a standardized sequence of postural changes with a defined procedure [Win05]:

- The test starts after the subject had been lying for 10 minutes
- Pulse and blood pressure are measured for 2 min in fixed intervals
- After standing up, pulse and blood pressure are measured immediately
- Measurement of pulse and blood pressure in fixed intervals for a duration of 10 min

The Tilt Table Test is widely accepted as gold standard method for automatized measurements of orthostatic reactions. The subject lies down on a tilt table which is being tilted at fixed time intervals between a horizontal and an $60 - 80°$ upright position. Throughout the whole measuring procedure, pulse and blood pressure are acquired. [Win05]

A big disadvantage of both tests is the clinical environment where the test is commonly proceeded. The physiological functions of the body are linked to psychological processes [Ber97]. Thus, just being at the hospital or to be at the doctor's leads to stress and agitation, which might influence the ***ANS***. This can potentially lead to increased heart rate and blood pressure and hence, to measurement errors in ***HRV*** analysis. As a result, the measured orthostatic reaction is different, in comparison to reactions after posture changes during daily life activities in a regular, well known environment. This phenomenon is also known as *white coat syndrome* [Owe99].

Chapter 4

Methods

The general goal of this bachelors's thesis is the replacement of the clinical Tilt Table Test through a system that makes unsupervised analysis of orthostatic reactions in a home monitoring scenario possible. Therefore, several requirements are needed: First of all, the system should be suited for a unsupervised detection of postures and posture changes in daily life activities. According to that, two ***IMU*** sensor units are necessary: one for the chest and another for the leg. Secondly, the system should be able to measure and evaluate the ***HRV*** during posture changes. For this, a chest-worn ***ECG*** sensor is used.

4.1 Data Acquisition

The evaluation of the developed algorithms was splitted up into two studies: ***HRV*** analysis and posture change detection. For the ***HRV*** analysis a sensor node, containing an ECG sensor, was used which recorded ***ECG*** data with a sampling rate of 250 Hz. For the ECG, one channel according to Lead II of Eindhoven's triangle was recorded. For that, the negative electrode was placed on the sternum whereas the positive electrode was placed on the left hand costal arch. To prevent electromagnetic interference, a third electrode was used according to the Driven-Right-Leg circuit (see Figure 3.1(b)). Based on this, HRV parameters were computed.

For posture change detection, the chest worn sensor additionally contained an ***IMU*** sensor with accelerometer and gyroscope, as well as a barometer. All data of the chest sensor were recorded with a sampling rate of 100 Hz. As leg sensor, the accelerometer of a regular off-the-shelf smartphone was used which had an inconstant sampling rate between 10-20 Hz.

To reject wrong posture events like stair climbing, the altitude changes are computed with the barometer data of the chest sensor. The data collection can be started and stopped with an Android

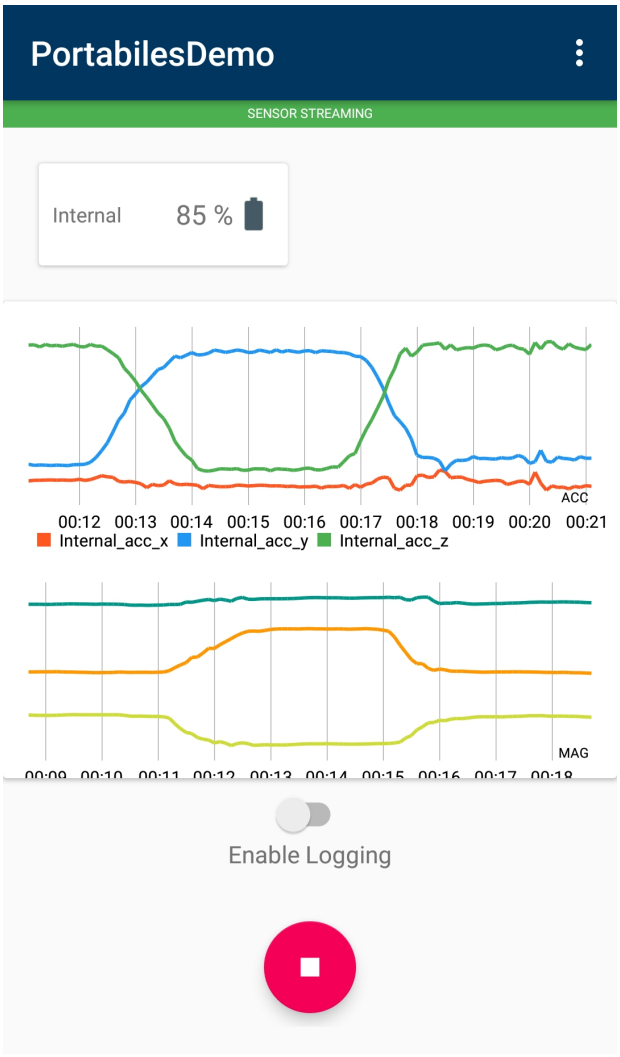

Figure 4.1: Screenshot of the Android based application for data recording

based application. The chest sensor transfers the data to the smartphone application via Bluetooth Low Energy. The acquired data from both, smartphone and chest-strap sensor, were stored in .csv files for further processing in Python. Figure 4.1 shows a screenshot of the application during streaming.

To develop an algorithm that is able to detect postural transitions, a small pre-study with five subjects was conducted. The study consisted of a randomized sequence containing different postures such as sitting, lying, standing and walking. All postures were performed in different variations like comfortable sitting or concentrated working at a writing desk. Furthermore, the changes in altitude were recorded.

4.2 Data Processing

For the following calculations the NumPy module of Python was used frequently. It provides a variety of functions for easy and fast computations directly on arrays [Num18].

4.2.1 Posture Change Detection

The focus of this bachelor's thesis was the correct detection of posture changes. The system should be able to detect following postures and the changes between them:

- Standing
- Walking (as a subgroup of standing)
- Sitting (in different postures, e.g. comfortable or at a table)
- Lying (in different postures, e.g. on the back or on the side)

To overcome the issue of different sampling rates, the data streams from both sensors were downsampled to 10 Hz.

The actual posture was detected by calculating the angle between the chest and the leg sensor in combination with a gravity vector analysis. To make home monitoring possible, it has to be considered that the mobile phone or the chest sensor can be placed in different orientations in the user's pocket or on the chest. Therefore, it is necessary to eliminate influences of these different sensor orientations. In order to compute the right angle independent of sensor orientations, a functional calibration approach was chosen which needs to be performed every time after the sensors were attached to the body. Functional calibration is a common and easy way to perform a sensor-to-body alignment and has been used multiple times in other works, such as [Pal14], [Fav09] and [Ros13].

For this work, the chest-worn sensor needs to be aligned to the chest and the smartphone to the leg. Therefore, two pre-defined movements were performed to calibrate the system: Firstly leaning the upper body to the front and back (chest alignment) and secondly, lifting the leg with the mobile phone stored in the in pocket and reverse (smartphone alignment).

The 3D acceleration vectors need to be in the same plane to compute the angle between chest and leg. For that reason, a ***Principal Component Analysis (PCA)*** was applied. The ***PCA*** is commonly used to analyze datasets and extract important information to represent it as a set of new orthogonal variables (the principal components), which are usually of lower dimensions than the original data. These components are sorted by the highest variance [Wil10].

To execute the ***PCA*** for the given data, the sample mean of each 3D acceleration vector in time has to be shifted to zero first:

$$\hat{a_i} = a_i - \bar{a_i},\ \forall_i = 0, ..., n \tag{4.1}$$

$$\text{with } \bar{a_i} = \frac{1}{n} \cdot \sum_{i=0}^{n} a_i \tag{4.2}$$

As next step, all vectors $\hat{a}$ are arranged as column vectors to a matrix A ($A \in (3 \times n)$). With this matrix the empirical covariance matrix C can be calculated as denotated in Equation 4.4 :

$$A = (\hat{a_0}, \hat{a_1}, ..., \hat{a_n},) \tag{4.3}$$

$$C = \frac{1}{n-1} \cdot AA^T \tag{4.4}$$

With the covariance matrix C the eigenvectors v_i and eigenvalues λ_i can be calculated. From that C can be rewritten as:

$$C = QWQ^T \tag{4.5}$$

Here, Q is a matrix containing the eigenvectors and W a diagonal matrix containing the eigenvalues, both sorted in descending order of the eigenvalues. As a last step, the acceleration vectors can be transformed into the new coordinate system with the principal components as new base (Equation 4.6).

$$y_i = Q^T \hat{a_i} \tag{4.6}$$

To distinguish between sitting and standing or lying, the angle between chest and leg sensor was computed. Thereby, the ***PCA*** was used to eliminate the 3rd dimension of the acceleration vectors of both sensors and to transform them into the same coordinate system, the mid-sagittal plane of the human body. To generate a 2D vector, the least significant axis of the transformed 3D acceleration signals was deleted. The sagittal plane of the human body is an anatomical plane

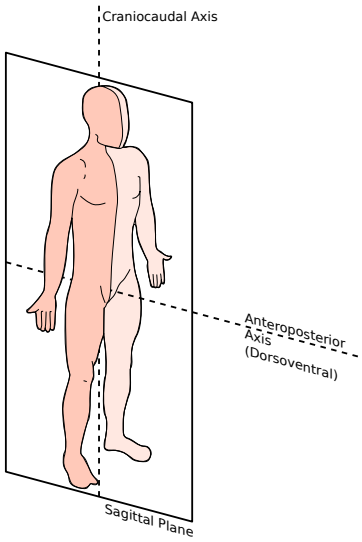

Figure 4.2: Schematic representation of the human's sagittal plane, *Source: Wikimedia Commons; Author: Edoardo:[Edo11]*

which divides the body into a right and a left part (see Figure 4.2). The start- and endpoints of the functional calibration part were labeled manually to perform the ***PCA***. Afterwards, all acceleration vectors can be transformed into the resulting coordinate system. The Figures 4.3, 4.4 and 4.5 illustrate the transformation pipeline from the raw to the transformed 2D data (**Blue:** Functional calibration movement, **Darkgray:** Standing, **Lightgray:** Sitting, **Green:** Lying).

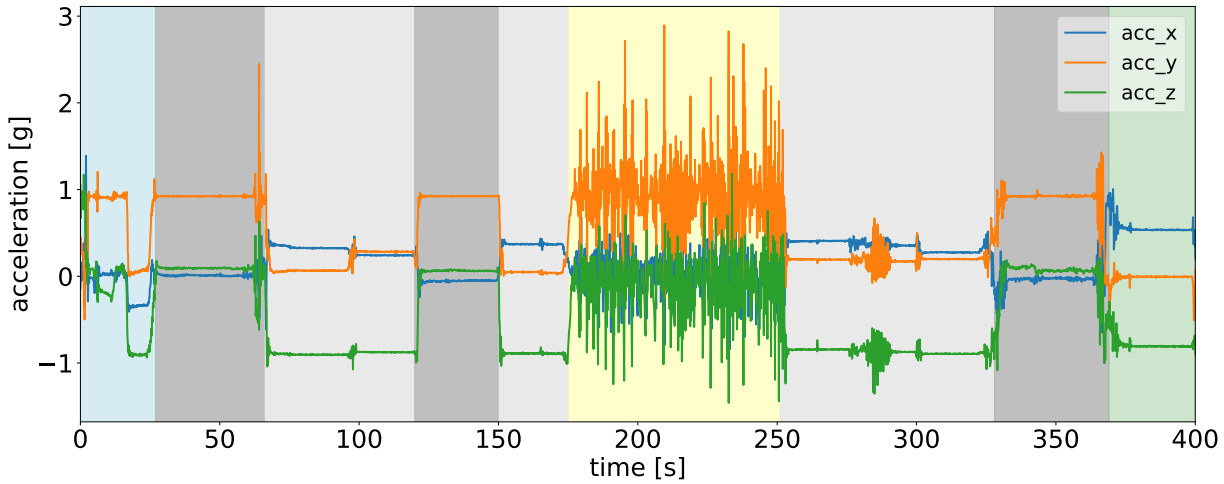

Figure 4.3: Accelerometer data of the mobile phone

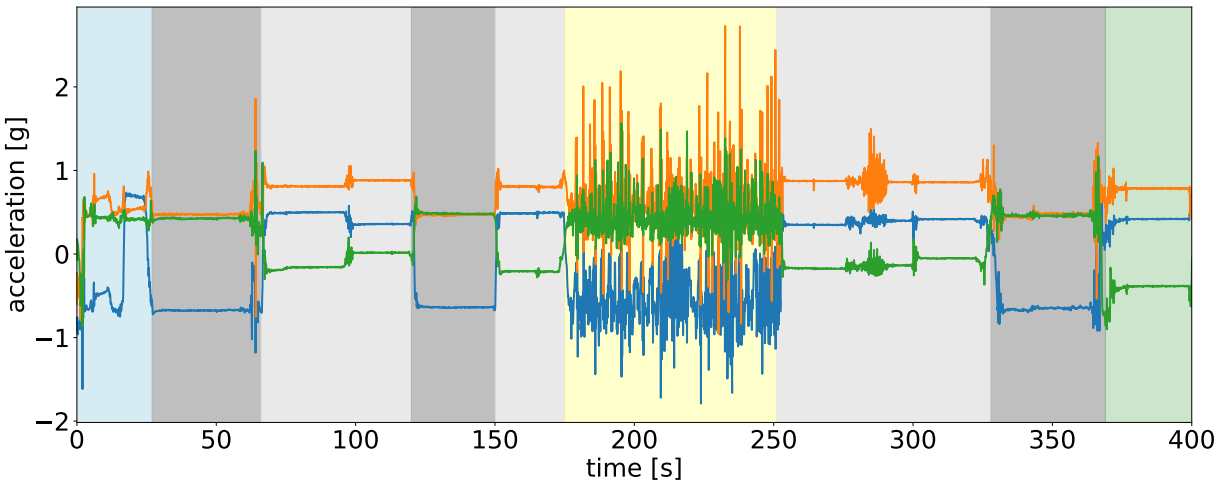

Figure 4.4: Transformed data after PCA

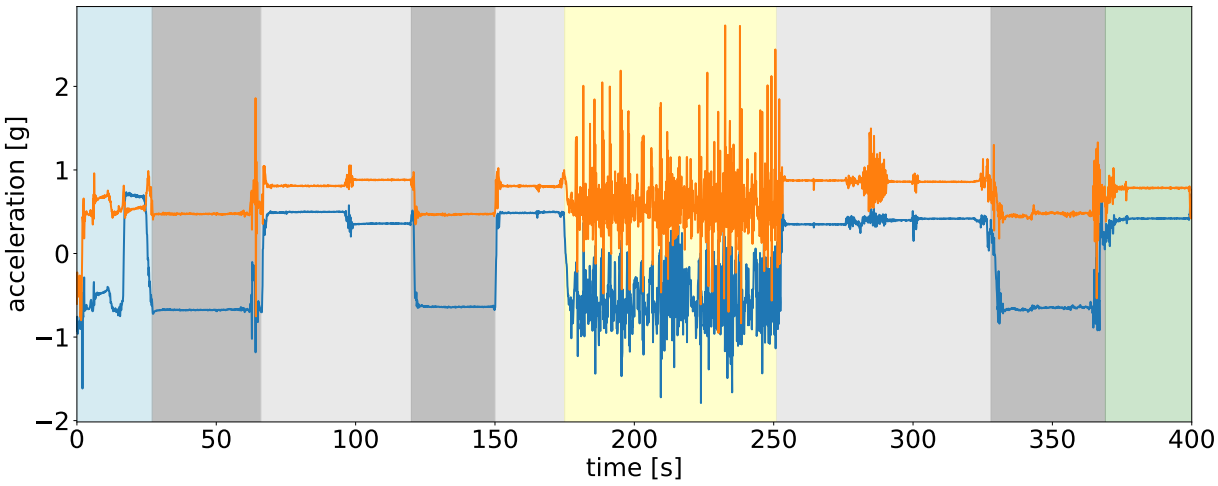

Figure 4.5: Transformed data after removal of least significant axis

Using Python, the whole PCA pipeline can be performed for 3D vectors with the sklearn module as sketched in Listing 4.1:

Listing 4.1: Transformation of acceleration data into new ***PCA*** coordinate system

```
1
2 from sklearn.decomposition import PCA
3 def PCA_calculation(vector_data, start, end):
4
5     #label start and endpoint of functional
```

```
    #calibration manually
    pca = PCA(n_components = 3)
    calibration_data = vector_data[start:end]

    #perform pca with calibration data
    pca.fit(calibration_data)


    transformed = list()

    #transform every vector in new coordinate system
    for vector in vector_data:
        transformed.append(pca.components_.dot(vector))


    return transformed
```

After transforming both 3D vectors into the same plane as 2D vectors, the angle between both vectors can be calculated, irrespective of how the sensors are orientated relative to the body (see Listing 4.2).

$$\theta = arctan(\frac{a \times b}{a \circ b}) \tag{4.7}$$

With the acquired data from the pre-study it was observed that especially the walking parts resulted in high angle variations. To minimize the noise, angle values were averaged over one second windows with 90 % overlap (see Figures 4.7 and 4.8). The angle is computed to determine wether the subject is is sitting, standing or lying. However the relative angle between both vectors is approximately the same for standing and lying and is only rotated globally by 90° (see Figure 4.6). Therefore, standing and lying need to be differentiated separately by comparing the current direction of the gravity vector with the direction of the gravity vector during the standing phase of the functional calibration step. The gravity vector is labeled partly automatic because the user has to set the start- and end point manually. If both gravity directions are aligned the current posture is classified as standing, whereas it is classified as lying if the directions differ from each other.

Listing 4.2: Angle calculation between the transformed acceleration data

```
def angle_calc(leg, chest):

    angle = []

    #dot product of the transformed vectors
    for chest_zip, leg_zip in zip(chest,leg):
        dot = np.dot(chest_zip, leg_zip)

    #angle calculation
    angle.append(math.degrees(np.arctan2(
    np.linalg.norm(np.cross(chest_zip, leg_zip)), dot)))


    return np.asarray(angle)
```

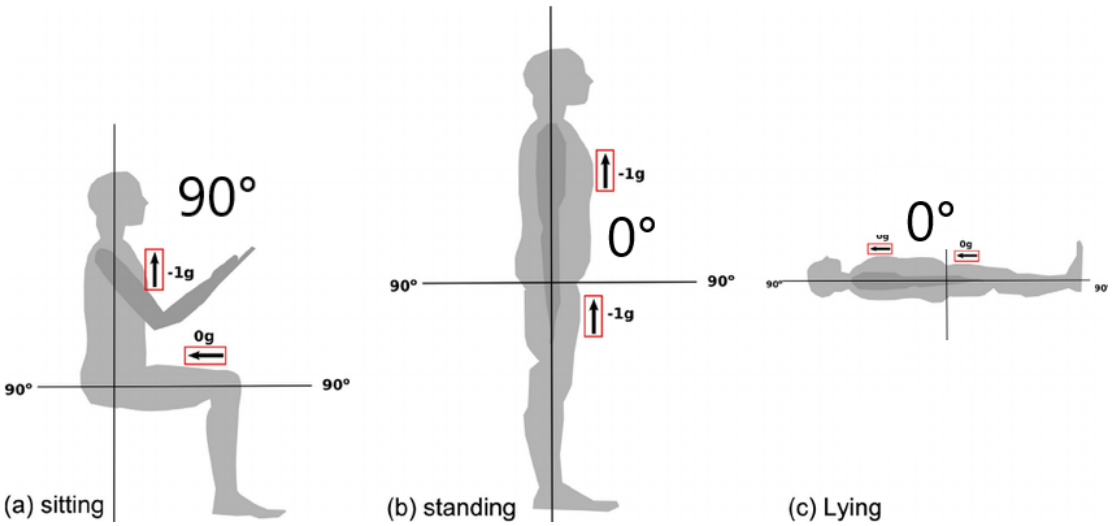

Figure 4.6: Different postures with their acceleration vectors and the corresponding angles between. *Modified from [Low14]*

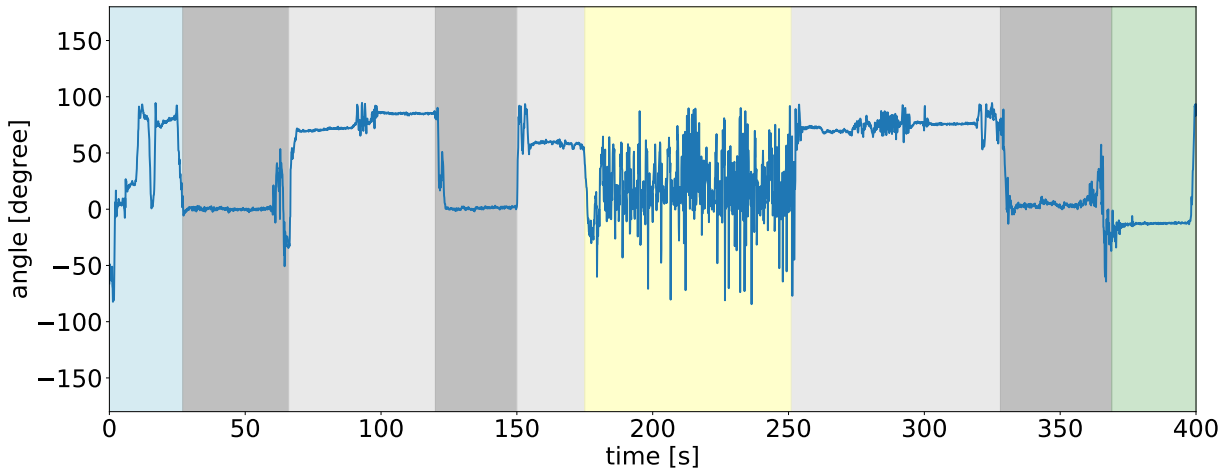

Figure 4.7: Raw angle between the transformed acceleration signals

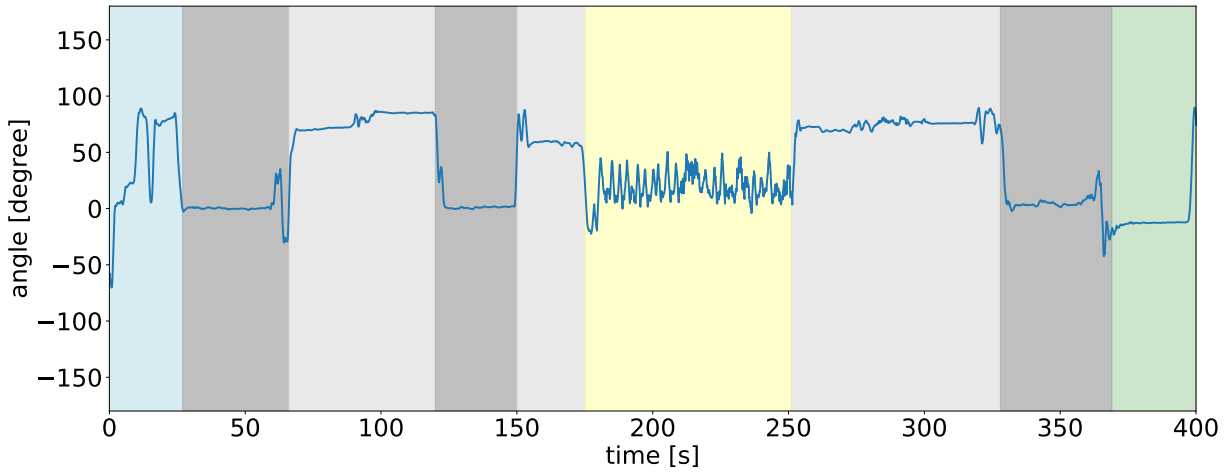

Figure 4.8: Averaged angle between the transformed acceleration signals

To make sure that there are no further influences on the change of heart rate, other than the orthostatic reaction some correctly detected posture change events need to be rejected in a home monitoring setting. For that, following rules were defined to remove posture events if:

- the subject is performing more intense physical activities other than walking, such as running
- the subject is climbing stairs
- the time difference between two posture events is $\leq$ 5 min

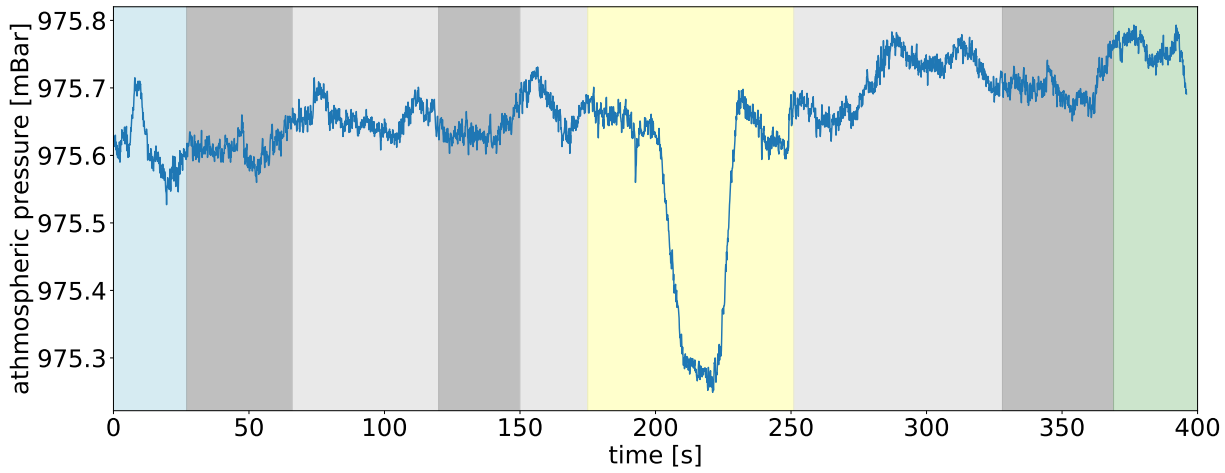

(a) Barometer Signal

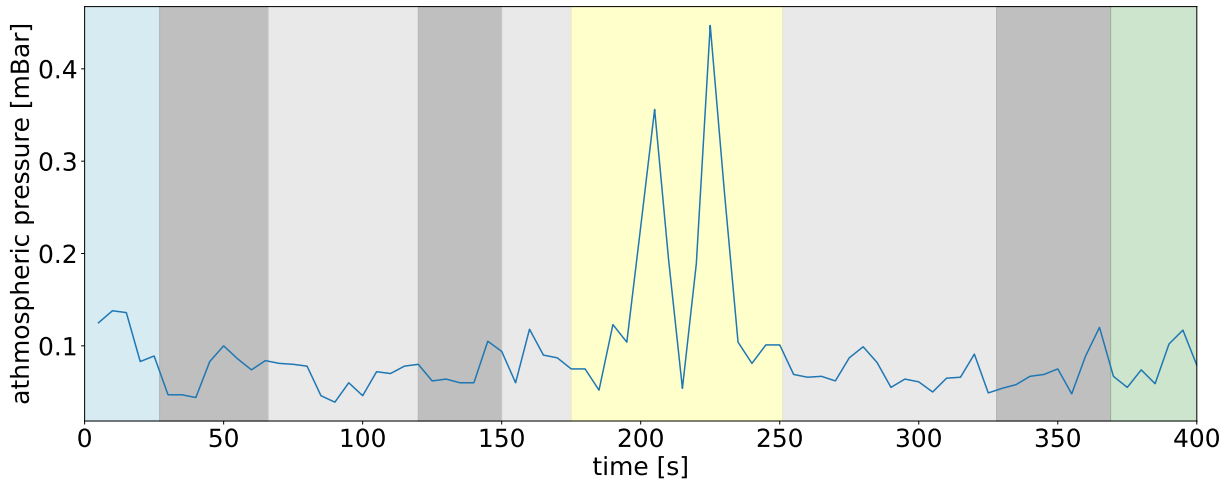

(b) Pressure Differences of 10s barometer windows with 50% overlap

Figure 4.9: Barometer data and windowed pressure difference

Therefore, a static angle detection was implemented which rejects all parts with high angle variance. For that, the variance was computed over rolling windows with a window size of 90 samples (see Equations 4.8 and 4.9. Every window with variances ≥ 300, a threshold which was empirically determined based on data from the pre-study, was rejected.

$$\bar{a} = \frac{1}{n} \sum_{i=0}^{n} a_i \tag{4.8}$$

$$\sigma^2 = \frac{\sum_{i=0}^{n}(a_i - \bar{a})^2}{n} \tag{4.9}$$

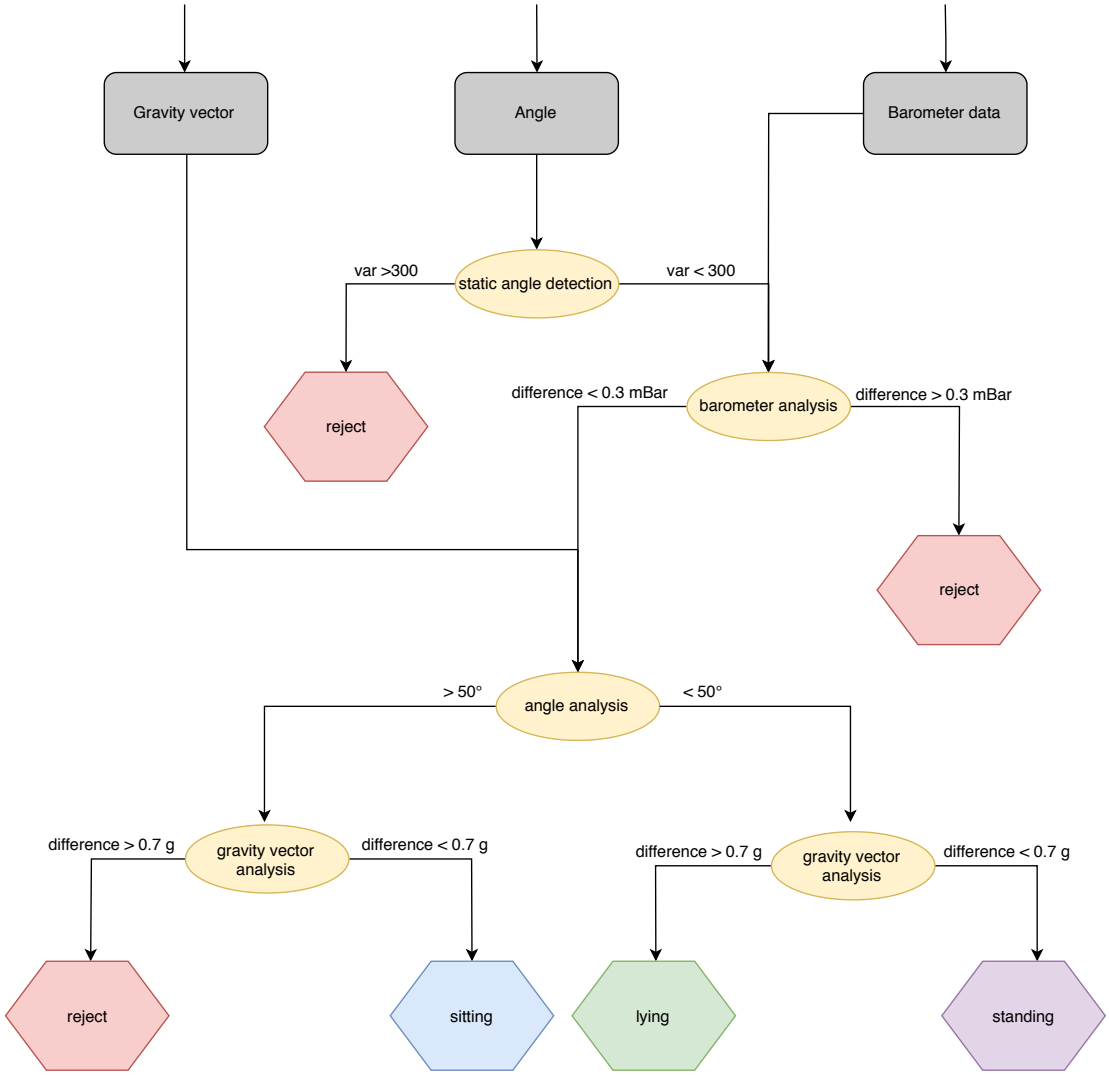

Figure 4.10: Decision Tree for the detection of postures

After angle analysis, it was observed that there were some incorrectly computed angle samples due to noise while walking. Since an output data rate of 10 posture samples per second is not necessary for a reliable posture change detection, data was downsampled to an output data rate of one sample per second. Therefore, data was divided into windows of one second with no overlap. The final posture values were then defined as the median values within the windows.

To detect stair climbing, values from the integrated barometer, which measures atmospheric

pressure in mBar, were used. If one subject is climbing stairs, and thus increasing the altitude, the atmospheric pressure decreases. In this work, barometer data was windowed over 10 seconds with 50% overlap. If the difference between the window's minimum and maximum value is higher than 0.3 mBar, which was empirically determined based on pre-study data, stair climbing is detected and the whole window is is rejected from posture analysis. Figure 4.9 shows the barometer data as well as the pressure differences per window.

As described in Section 3.3 the orthostatic reaction is usually divided into different phases. Because the circulatory system needs some time to adapt to posture changes, there should not be more than one posture change within a window of five minutes for a reliable analysis of the orthostatic reaction. Therefore, all posture changes measured within five minutes after a valid posture change are not valid for the for ***HRV*** analysis and will be rejected [Wie09]. The decision tree in Figure 4.10 depicts the rules that were implemented for posture detection. Figure 4.11 shows the result of the posture detection for one dataset acquired in the study. The rule that every posture should only be detected as valid if it is held for more than five minutes was excluded in here because the study conditions did not allow a long term evaluation.

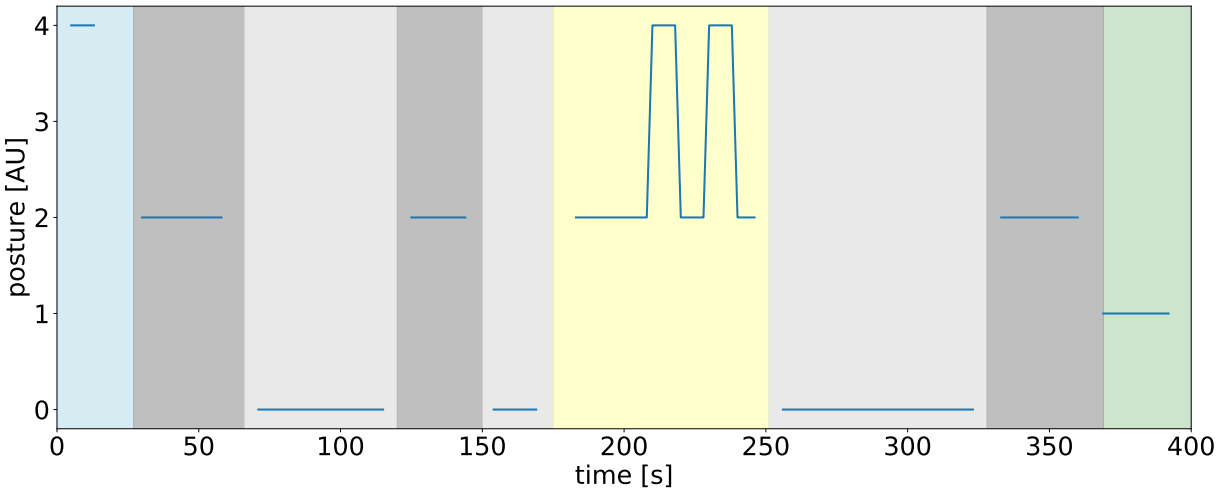

Figure 4.11: Detected postures depicted in a discrete way: 0 = sitting, 1 = lying, 2 = standing, 3 = stair climbing (to reject), no data = rejected because of the static angle detector

4.2.2 HRV Analysis

For the ***HRV*** analysis the acquired ***ECG*** data is first filtered before an algorithm for R-peak detection is applied. For R-peak detection an algorithm proposed by Hamilton et al. [Ham02], which is included in the BioSPPy Python module was chosen [dT]. It combines filtering the raw

ECG signal with a high sensitivity R-peak detection. This is important for a correct calculation of the subject's heart rate variability. Figure 4.12 shows results from the R-peak detection for an example ***ECG*** signal. After P-peak detection the ***HRV*** measures were computed based on the descriptions of [Ric16] and [Sch99]. Table 4.1 lists the extracted features. They can be divided into two parts:

- time-domain features
- frequency-based features

Table 4.1: Selected measures for HRV analysis

	Description	**Unit**
AvgRR	Average of RR intervals	ms
StdRR	Standard deviation of RR intervals	ms
AvgSD	Average of successive differences	ms
StdSD	Standard deviation of successive differences	ms
RmsSD	Root mean square of successive differences	ms
pRR20	Number of successive differences $\leq$ 20 ms divided by all RR intervals in the window	%
pRR50	Number of successive differences $\leq$ 50 ms divided by all RR intervals in the window	%
LF/HF	LH/HF ratio – low frequency power divided by high frequency power	

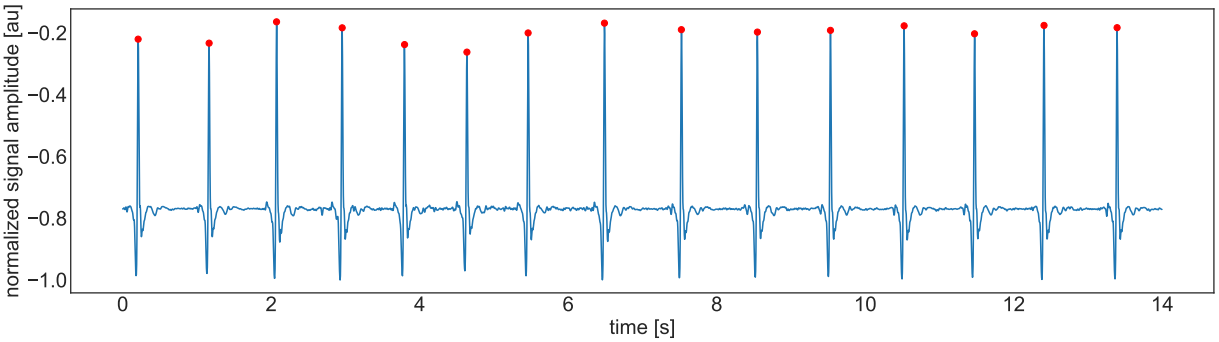

Figure 4.12: R-peak detection

To perform the *HRV* analysis, following time-based features were implemented:

- **RR Intervals:** RR intervals are computed as the time difference between two consecutive R-peaks as returned by the R-peak detection algorithm. Additionally, as presented in Figure 4.13, average and standard deviation were calculated over 10s windows with 90% overlap. If one R-peak was not detected by the algorithm this would result in drastically higher or shorter RR intervals. For that reason, RR intervals smaller than 500 ms (corresponding to a heart rate of 120 bpm) or bigger than 1100 ms (corresponding to a heart rate of 54 bpm) were set to the value of the precedent RR interval.

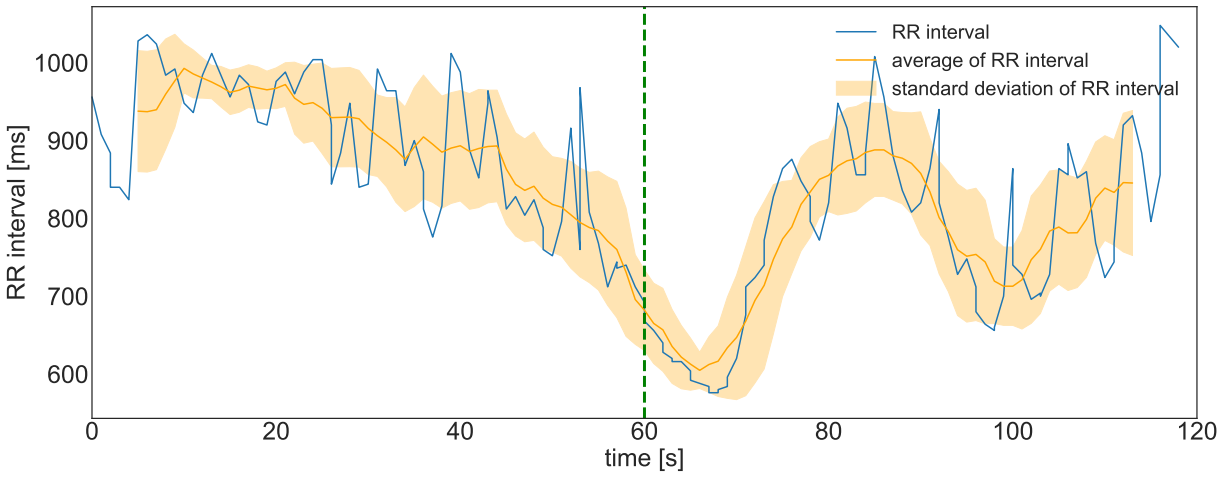

Figure 4.13: RR interval with average and standard deviation; **green, dashed:** Stand-up event

- **Successive Differences:** This measure represents the time difference between two consecutive RR intervals. Similarly to the RR intervals, the average and standard deviation of the successive differences, as well as the root mean square was calculated over 10s windows with 90% overlap (see Figure 4.15).

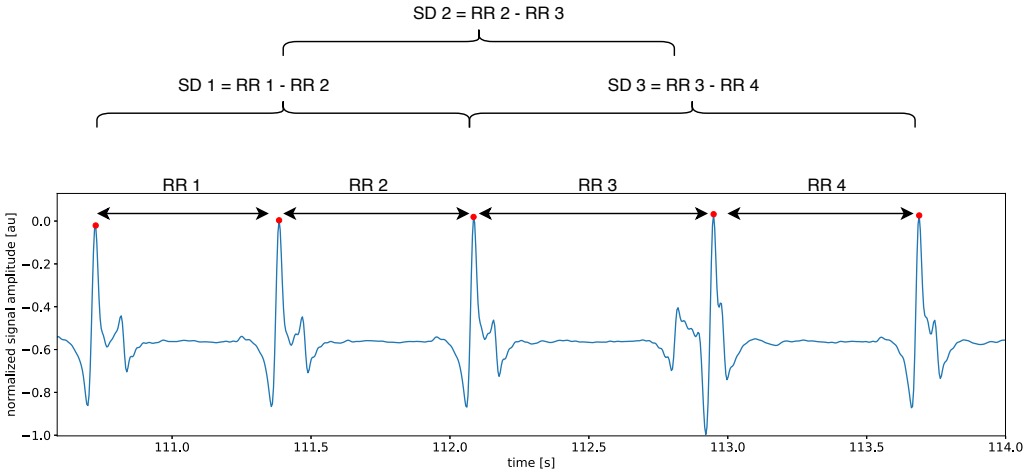

Figure 4.14: Computation of RR intervals (RR) and successive differences (SD)

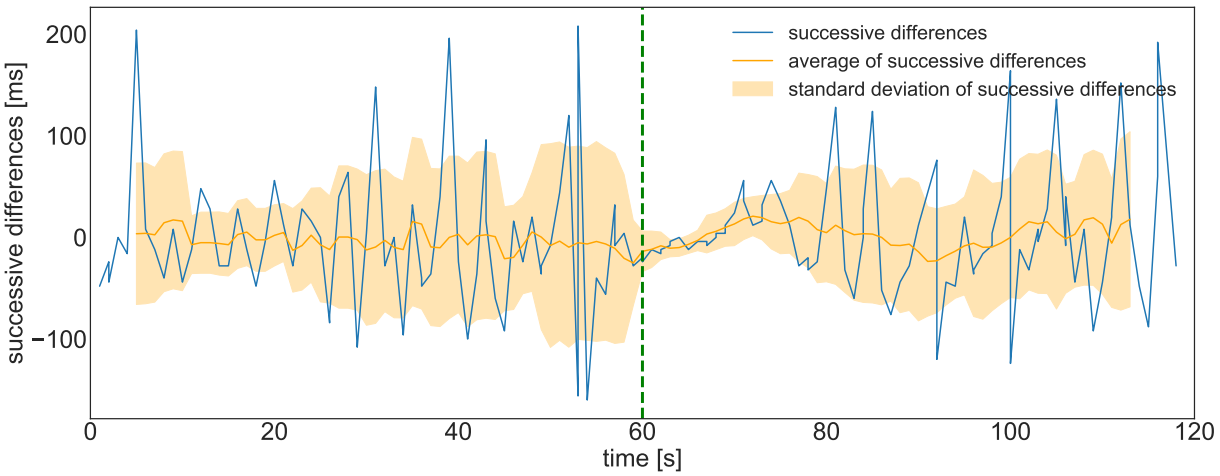

Figure 4.15: Successive differences between consecutive RR intervals; **green, dashed:** Stand-up event

- **Number of successive differences over a threshold divided by all RR intervals in the window given in percent:** This feature was calculated with thresholds of 20 and 50 ms. The calculation was performed in 10 s windows with 90% overlap (see Figure 4.16).

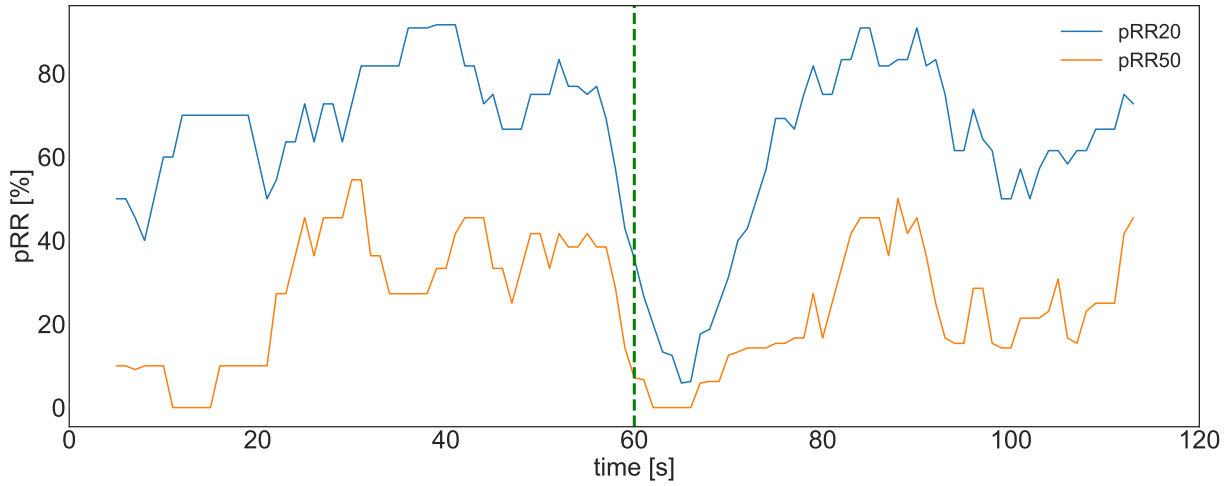

Figure 4.16: Number of sucessive differences over a threshold in %; **green, dashed:** Stand-up event

As frequency-based approach, only one characteristic was computed:

- **Power spectrum:** For the computation of frequency-based measures Welch's averaging method for estimating the spectral density of the RR intervals was used [Wel67]. For computing the periodogram (an estimate of a signal's spectral density), the signal was divided into windows with 64 seconds length and 50 % overlap. The resulting spectral density can be divided into different segments based on the frequency: ***very low frequency (VLF)*** (<0.4 Hz), ***low frequency (LF)*** (0.04 Hz - 0.15 Hz) and ***high frequency (HF)*** (> 0.15 Hz). Figure 4.17 shows an example for a power spectrum of a subject at rest and during a 90° head-up tilt. As measure to evaluate the orthostatic reaction, the LF/HF ratio which describes the balance between sympathetic- and parasympathetic nervous system, was selected [Sch99].

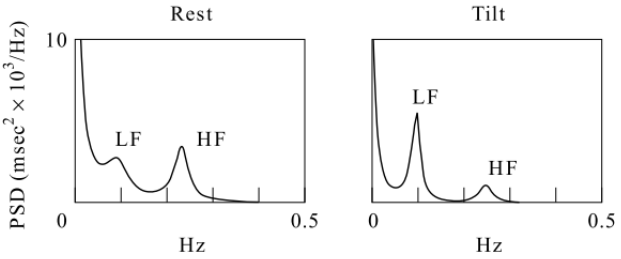

Figure 4.17: Power spectrum of a subject at rest and 90° head-up tilt [Sch99]

Chapter 5

Evaluation

The evaluation of the presented work is twofold: Firstly, the correct detection of valid postural transitions was examined in order to evaluate if the accuracy is high enough to establish home monitoring. Secondly, it was analyzed which of the implemented measures for ***HRV*** analysis are suited best for assessing and quantifying the orthostatic reaction. Therefore, two independent studies were conducted. All data were acquired at the facilities of the Machine Learning and Data Analytics Lab (Erlangen, Germany).

5.1 Posture Change Detection

For the study to evaluate the posture change detection algorithm 18 healthy subjects (10 male, 8 female) were acquired. The data was recorded with two subjects (and two study personnel) simultaneously. Because the utilized smartphones experienced technical problems which were discovered during data analysis, several data recorded of this mobile phones (8 subjects) had to be rejected. To overcome the condition of less study participants, a second study with the same study protocol was conducted with 6 subjects. Additional information about the remaining study participants are shown in Table 5.1.

Table 5.1: Information about the 10 participants. All values are given as mean $\pm$ SD

Gender	Age in yr	Height in cm
6 male, 4 female	26.6 ± 2.94	175.2 ± 11.06

All participants were asked to perform a sequence of different tasks in different postures. To account for different sitting positions, multiple chairs with different properties were used (see Figure B.1). Because of the variety of different tasks in the study protocol, no task was performed

for longer than 30 s. Therefore, the heuristic rule which rejects all postures held for less than five minutes was not included in the evaluation.

The chest sensor was attached to the subjects's clothing with a double-sided tape (see Figure 5.1), the smartphone was placed in the right or left trouser pocket.

Figure 5.1: ***IMU*** sensor attachment to clothing for study

The study protocol consisted of the following tasks, which were performed in a fixed order:

- **Task 1: Start and functional calibration**
  Before data acquisition the sensor was attached to the subject's chest by the study personnel. Afterwards, data recording was started and the smartphone was placed in the trouser pocket. As next step, the functional calibration for the sensor-to-body alignment was performed. The duration of the functional calibration was about 15 s.

- **Task 2: Standing**
  After functional calibration was done, the subject was instructed to keep standing for another 30 s.

- **Task 3: Comfortable sitting with armrests**
  This task consisted of sitting comfortably on an office chair with armrests for about 30 s. The chair was blocked from leaning back. This should simulate a situation in daily life in which the subject might sit in a lecture or a meeting.

- **Task 4: Upright sitting with armrests**
  Next, the subject was asked to sit on the same chair but it should lean forward towards a writing desk. This should simulate activities in a home environment like learning, concentrated working or eating at a table. The subject had to sit there for 30 s either.

- **Task 5: Standing**
  After these sitting tasks the subject was asked to repeat standing upright for 30 s.

- **Task 6: Sitting with leaning far back**
  Then, the subject had to sit down on the office chair again, with the difference that the lean back function was unlocked. This should simulate a comfortable situation in a home environment like watching TV or reading a book. It has to be mentioned that the used chairs were unexpectedly hard to lean back, so some subjects were not able to reach the full range of leaning back.

- **Task 7: Walking and stair climbing**
  The next task was to walk to the lab facility's coffee kitchen. This included a longer walk distance as well as climbing stairs. After reaching the coffee kitchen, the subject had to walk back to the study room with the provided chairs. The walking and stair climbing part should simulate tasks and situations of daily living in a home environment.

- **Task 8: Comfortable sitting without armrests**
  Back at the study room, the subject had to sit down again for 30 s on a simple chair without armrests. Thereby it should lean back and simulate sitting in a lecture or meeting like in Task 3.

- **Task 9: Upright sitting without armrests**
  Afterwards, sitting at a writing desk was simulated again using the chair without armrests. The duration of this task was 30 s.

- **Task 10: Standing**
  Then, the subject was asked to repeat standing for another 30 s.

- **Task 11: Lying on the back**
  To include all postures the algorithm should be able to detect, the subject had to lie down on the back simulating sleeping or lying on a sofa. Therefore, a table in the study room was provided. This task also took 30 s.

- **Task 12: End of data acquisition**
  The study protocol was concluded by instructing the subject to stand up for a few seconds and returning the mobile phone. At the end, the data recording was stopped.

To evaluate the algorithm, all postures were labeled manually with the raw data to distinguish lying, sitting, walking and standing. This ground truth data was then compared to the output of the posture detection algorithm sample by sample. Because the duration of posture changes is not of significant importance for the detection, samples with no detected posture directly before and after a postural transition were excluded in a second step.

Because the study should not take too much time, the rule that no additional posture changes should be allowed within five minutes after a detected posture change was not considered. Instead, the detection timeout was set to 10 s. This should prevent a wrong detection of posture changes

because of short time fluctuations in posture data. If the posture was not held continuously for this time, every associated posture change was deleted. If every requirement of a posture change is fulfilled, this event is accepted as valid. The exact timestamp of that posture event was set in the middle between the endpoint of the first and the startpoint of the second posture.

As last part of the evaluation of this algorithm, the correct rejection of stair climbing events had to be assessed. Therefore the number of rejected stair climbing events was compared to the study protocol which mentioned two events. Stair climbing to the first floor and back to the ground level afterwards.

5.2 HRV Analysis

To estimate which features are best to assess the functionality of the ***ANS***, a study with 12 healthy subjects (7 male, 5 female) was conducted. Because of problems during data acquisition which resulted in unusable data, two datasets had to be excluded from analysis. Additional information about the characteristics of the remaining study participants are shown in Table 5.2.

Table 5.2: Information about the 10 participants. All values are given as mean $\pm$ SD

Gender	Age in yr	Height in cm
5 male, 5 female	24.7 ± 4.94	171.5 ± 10.17

The calculated features of the ***HRV*** analysis are described in Subsection 4.2.2.
The study consisted of one sit-to-stand transition event which should trigger an orthostatic reaction. The electrodes for ***ECG*** recording were attached according to Lead II of Einthoven's triangle (for a closer description see Section 3.1).

At first, the participants were asked to sit down on a chair so that the cardiovascular system can adapt to the current posture. After the participants have been sitting for at least five minutes, the ***ECG*** recording started. After one minute of ***ECG*** data acquisition the subject was advised to stand up and keep standing for another minute. After this period of time the data acquisition was stopped (see Figure 5.2).

In order to determine the best performing ***HRV*** measures the dataset was divided into two parts before and after the posture change, respectively. Both parts had a duration of 60 s each. Start- and endpoint of the data processing was labeled manually so that the posture event happened after exactly 60 s. The computed ***HRV*** measures were averaged for the data before and after the posture change, resulting in two values per ***HRV*** measure. For evaluation of the best performing

measures for orthostatic reaction, the relative changes of the ***HRV*** measures during the sit-to-stand transition was computed in percent.

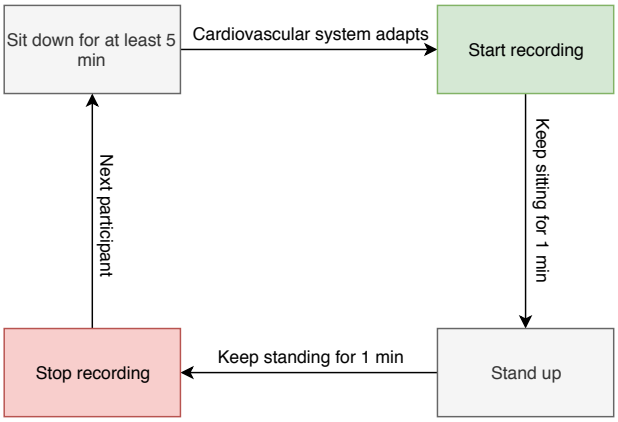

Figure 5.2: Study protocol for evaluation of orthostatic reaction

Chapter 6

Results

6.1 Posture Change Detection

Accuracy of detected postures:

As shown in Table 6.1, the classification of *sitting* achieved the highest accuracy (82.22 %). In contrast, *standing* was classified correctly for 77.63 % of the samples whereas *lying* achieved the lowest accuracy with 67.99 %. In total, 78.77 % of the posture samples were detected correctly.

Table 6.1: Accuracy of posture detection per sample

Posture	**Accuracy**
Standing	77.63 %
Sitting	82.22 %
Lying	67.99 %
Total	78.77 %

Figure 6.1 presents a confusion matrix of the posture change detection. It is remarkable that in 79.8 % of the falsely detected samples the algorithm detected *no posture*.

Figure 6.1: Confusion matrix of detected postures

Accuracy of detected postures without samples rejected during posture changes:

The main difference to the aforementioned results is that only the *no posture* samples which happened *during* a posture are count. All samples from that class which were detected directly before, after or during a postural transition were taken out. Figure 6.2 depicts the resulting posture of a subject during task 8 and 9 of the study protocol. The correct detected samples are marked green. The red marked samples happened during the *standing* posture and need to be mentioned, whereas the blue marked samples can be rejected for analysis. This leads to a considerable increase in accuracy. Table 6.2 shows that every sample of *lying* was detected correctly whereas *sitting* and *standing* achieved accuracies of 94.20 % and 90.53 %, respectively.

Table 6.2: Accuracy of posture detection per sample (without *no posture* samples during posture changes

Posture	**Accuracy**
Standing	94.20 %
Sitting	90.53 %
Lying	100.00 %
Total	92.93 %

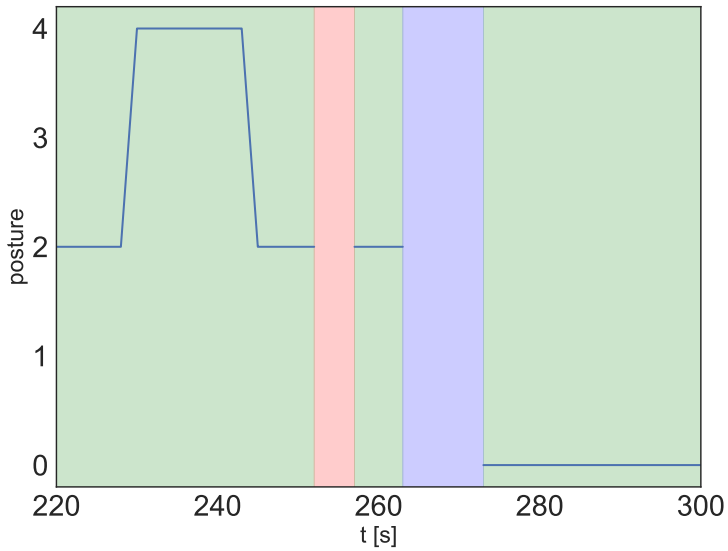

Figure 6.2: Visualization of the rejection of *no posture* samples during postural transitions

Figure 6.3 depicts the distribution of the detected samples as confusion matrix. It can be seen that there are 89.79 % less *no posture* samples in contrast to Figure 6.1. Only 28.78 % of the falsely detected samples are *no posture* samples, compared to 79.8 % in Figure 6.1.

Figure 6.3: Confusion matrix of detected postures without *no posture* samples during posture changes

Accuracy of detected posture change events:

Table 6.3 shows the accuracies of detected posture changes. The postural transitions are divided into *stand-to-sit*, *sit-to-stand* and *stand-to-lie* transitions. Results show that *stand-to-lie* transitions were correctly detected in 86.67 % of the events, whereas *sit-to-stand* transitions were correctly detected 73.33 % of the time. *Stand-to-lie* transitions showed the best results with a correct detection in 90.00 % of the cases. In the whole measurement, which consisted of 70 postural transitions, only one transition was detected wrongfully (*sit-to-stand* detection even though the subject remained *seated*).

Table 6.3: Accuracy of posture change detection: **StSi:** Stand-to-sit transition, **SiSt:** Sit-to-stand transition, **StLy:** Stand-to-lie transition

Posture change	detected	not detected	total	accuracy
StSi	26	4	30	86.67 %
SiSt	22	8	30	73.33 %
StLy	9	1	10	90.00 %
Total	57	13	70	81.14 %

The last point of the evaluation was to assess the detection of *stair climbing* based on altitude changes. Therefore, the study design contained *stair climbing* up to the first floor and back. Results show that 90 % of the *stair climb* events were correctly detected (see Table 6.4).

Table 6.4: Distribution of correctly detected *stair climbing* events

	detected	not detected	total	accuracy
Stair climbing	18	2	20	90.00 %

6.2 HRV Analysis

The change of the different ***HRV*** measures during posture change are listed in Table 6.5. The values are denoted as mean $\pm$ standard deviation over all subjects. Results show that the *LF/HF* ratio showed the largest increase by far (918.10 %). However, the standard deviation is also very high (1203 %). Analyzing the time-domain features, it can be observed that only the standard deviation of RR intervals *StdRR* increased whereas the remaining measures were decreasing. The most distinct measure is *pRR50* with a decrease of 60.97 %. Nevertheless, all measures show a clear reaction of the ***ANS*** to a posture change.

Table 6.5: Change of HRV measures during posture change

	Change [%]
AvgRR	-9.56 ± 6.29
StdRR	$+53.75 \pm 62.45$
AvgSD	-41.77 ± 15.14
StdSD	-29.55 ± 24.88
RmsSD	-32.10 ± 18.33
pRR20	-34.85 ± 18.75
pRR50	-60.97 ± 22.29
LF/HF	$+918.10 \pm 1203$

Figure 6.4 presents boxplots of the ***HRV*** parameters before and after stand-up event. The central mark visualizes the median whereas the upper and lower endings of the box stand for the 25th and 75th percentile of the dataset. The whiskers describe the minimum and maximum of the values which were not considered as outliers. If there were any outliers, they are shown as dots. It can be observed that all computed features show a clear change after the postural transition. The boxplots reveal that the ***HRV*** measures *RmsSD*, *pRR50* and *LF/HF* show higher variance compared to other measures.

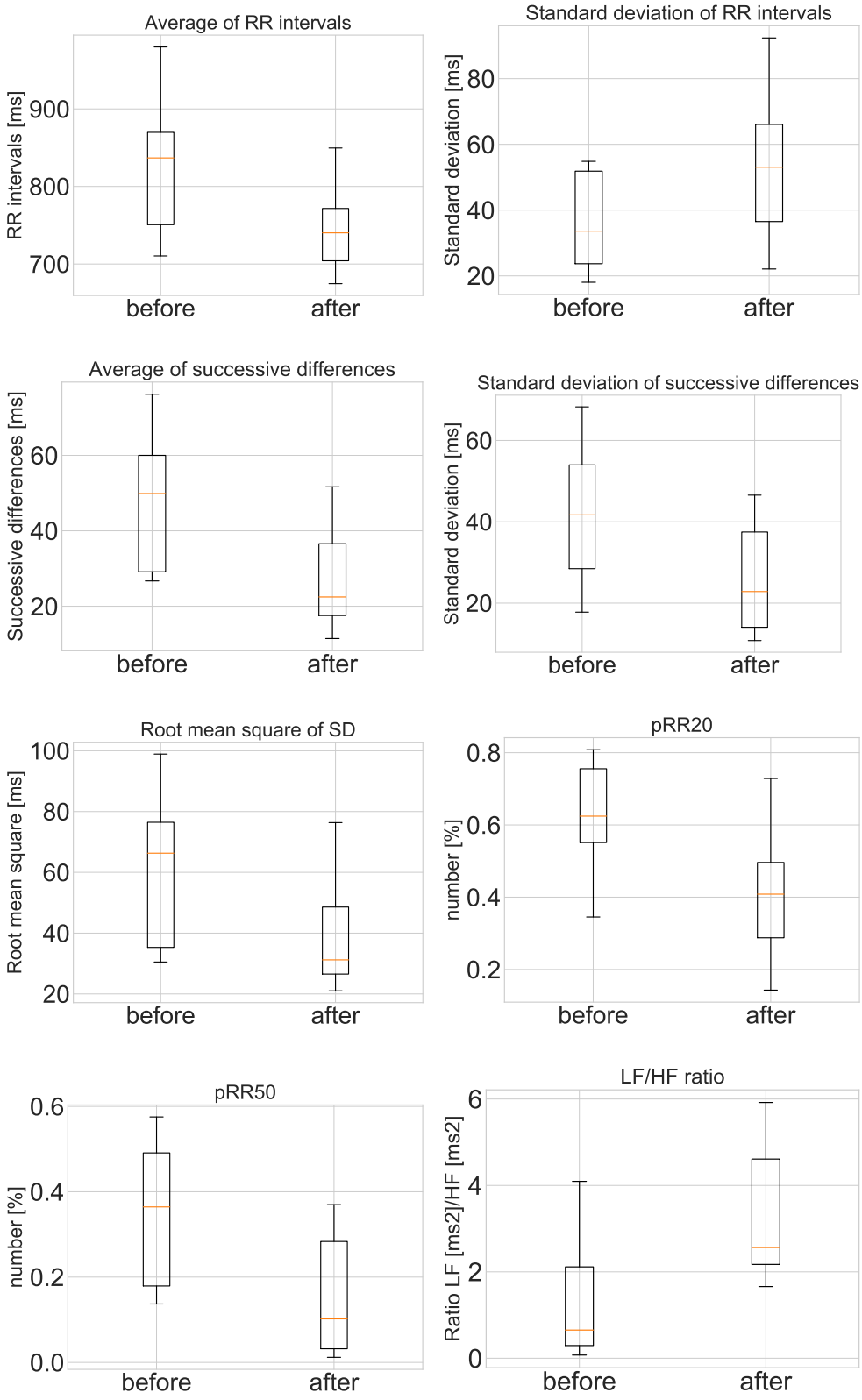

Figure 6.4: Boxplots to visualize the change of the HRV measures after posture change

Chapter 7

Discussion

The presented methods in this work were used to design an application that makes unobtrusive home monitoring of ***ECG*** data for ***HRV*** analysis possible. The main goal therefore was the correct detection of postures and the changes between them. The following Chapter discusses the presented methods and their corresponding results according to their suitability for a home monitoring application.

7.1 Data Acquisition

To measure the actual posture, a regular off-the-shelf Android smartphone, in combination with a chest sensor, was used. During the acquisition of test and study data it was observed that the proposed setup experienced some drawbacks. The first observation was that modern female fashion has front pockets that are too small for a regular smartphone, or in worst case, have no front trouser pocket at all. This might lead to the problem that the smartphone (and hence also the sensor) is placed in a wrong way or can not be placed at all. One possible solution could be another ***IMU*** sensor node, similar to the one used as chest sensor, which would be attached to the leg. In this case the smartphone would loose its part as sensor node and would only be used to run the application and log data acquired by the sensor nodes and streamed via Bluetooth Low Energy. Furthermore, this would also eliminate issues with the unstable sampling rates of the internal smartphone sensors. The changes in sampling rate are likely to be caused by the Android operating system which does not allow a low-level access to the internal sensor control. Even though a fixed sampling rate was requested by the sensors API, some internal power management optimizations might autonomously change the sampling rate in order to save power.

During the analysis of ***HRV*** parameters it was observed that the ***ECG*** sensor had a vulnerability in incorrect R-peak detection at posture events. Hence, R-peaks missed by the detection algorithm would lead to wrong ***HRV*** measures. Therefore, upper and lower thresholds for RR intervals were defined and samples were corrected if they were out of threshold bounds. Furthermore, some ***ECG*** signals were flipped because of wrong electrode placements. However, since the R-peak detection algorithm still worked reliably, this presumably had no impact on the data processing.

7.2 Data Processing

7.2.1 Posture Change Detection

As apparent from the results of the posture change detection study, the overall accuracy is 78.77 % due to the high number of *no posture* samples. Because a lot of movement happens during a posture change, the static angle detector removes parts of the postural transition. In addition to that, some problems with unstable sampling rates of the smartphone occurred which had an unknown origin. Because the problem first appeared shortly before the start of the study (and not during the pre-study), it could not be solved anymore by adapting the algorithm. Since the algorithm was only designed for stable sampling rates, the datasets had to be downsampled manually which led to a non-optimal alignment of the chest and leg sensors, leading to more *no posture* samples during posture changes.

The lowest accuracy (67.99 %) was noticed at the detection of *lying*. This can be explained by a longer transition time from *standing* to *lying* in comparison to the other posture changes. Furthermore, *lying* on the back took place at the end of the study protocol. Hence, effects of wrong sensor synchronization due to manual downsampling might had a higher impact.

For future work it is necessary to solve the problem of inconstant sampling rates. One possible solution would be adapting the downsampling procedure in the algorithm by including information from the sample timestamps. A second approach would be the use of an optimized streaming application which is able to set the sampling rate of the smartphone to a stable value.

Another point to mention is that postures in daily life are often held much longer than the 30 s in the study design. This leads to less *no posture* samples during posture changes compared to the total amount of recorded samples. Thus, it is possible to optimize the results by taking out the *no posture* samples which are happening during a posture change. As a result, a considerably higher accuracy of 92.93 % over all measured postures was achieved. Through the optimization, all relevant *lying* samples were detected correctly whereas the accuracy of *sitting* and *standing* increased as well. However, samples that were rejected while keeping a posture were still

considered as „wrongly detected“ and therefore lower classification performance. These results reflect a better view on the posture detection performance of the proposed algorithm in long term measurements.

The results from the posture change detection evaluation show an overall detection rate of 81.14 %. Most of the posture changes that were not detected were caused by too much activity before or after the posture change. As a consequence, there were incorrectly rejected samples during the new or the previous posture. If the high activity occurred during the walking or stair climbing part, it is possible that the participant walked at a faster pace.

To increase the accuracy of correctly detected posture changes, it would be possible to increase the window size for the posture sample smoothing to e.g. five seconds. However, this would also lead to information losses about incorrect movements with a short duration. Additionally, a study design with longer posture durations would be needed.

The developed system is designed to enable long-term monitoring of posture changes in a home environment. Over the whole day, multiple posture changes typically happen. In order to collect ***ECG*** data that is valid for ***HRV*** analysis of the orthostatic reaction it is important that the algorithm only selects the best fitting posture changes.Therefore, from a clinical point of view, it is not necessary to detect all posture changes correctly as long as the detected posture changes are valid for ***HRV*** analysis.

To align both sensors to the body, a functional calibration was performed. It was observed that performing the functional calibration more accurate considerably improved the results. Because the first study took place in a lesson where two subjects performed the study protocol simultaneously, there was less time to explain the functional calibration movements properly. For that reason, some subjects performed the calibration inaccurately. This resulted in a lower accuracy throughout all recorded measurements compared to the second study part, where a separated data acquisition with more clear and more detailed instructions was conducted.

To differ between *lying* and *standing*, the current gravity vector was compared to the gravity vector acquired during the *standing* phases of the functional calibration. This part had to be labeled manually according to the raw data. A possible improvement would be an automatic detection included into the functional calibration part.

Physically demanding activities are a strong influence on the change of the ***HRV*** parameter [Lan07]. Therefore, actions like running were already rejected by the static angle detector. To reject slower, but also exhausting activities like stair climbing, data from the barometer was used to determine altitude changes. It was noticeable that climbing the stairs too slowly could cause the algorithm to detect no stair climbing event. This is supported by the fact that only ascending

stairs, which is typically slower than descending stairs, were not correctly detected. Nevertheless, the evaluation of the study data yielded an accuracy of 90 %.

The study design only contained one stair climbing event in the lab facilities. In daily life, a subject would possibly climb multiple types of stairs with different altitude differences per day. Future work should therefore further test the robustness of the algorithm.

7.2.2 HRV Analysis

To evaluate the orthostatic reaction of the ***ANS*** as response to a posture change, ***ECG*** data was recorded and ***HRV*** analysis was performed. Regarding the computed time-domain methods, it is visible that only the standard deviation of RR intervals increased whereas all other parameters decreased. The heavy decrease of the time between two R-peaks leads to a increase in standard deviation of RR intervals by 53.75 %.

All features which are associated with the successive differences declined. Because the ***ANS*** has to constantly increase heart rate within a short period of time in order to maintain the blood supply to the brain, the successive differences and their variability are lower after a posture change compared to resting phases. Even though all features show a clear reaction of the ***ANS***, the *pRR50* feature showed the highest decrease by 60.97 %.

As frequency-based feature, the *LF/HF* ratio was computed. Posture changes induced a change in this parameter that was more than 15 times higher compared to the most distinct time-domain feature (918.10 % vs. 60.97 %). However the results show such a substantially high change, it has to be mentioned that the standard deviation is higher than the measured value. This indicates high inter-subject variations. As an accepted standard in literature it is recommended to record at least five minutes of ***ECG*** data to obtain sufficient data for a precise analysis of frequency-based analysis of ***HRV*** measures [Sch99]. It is also mentioned that a minimum of one minute recording is necessary for an accurate assessment of the *HF* component, whereas approximately at least two minutes are needed to address the *LF* component. To analyze the whole frequency range, including ***ultra low frequency (ULF)***, ***VLF***, ***LF***, and ***HF***, a 24 hour recording is recommended [Sch99].

Because the study design only intended one minute of *sitting* and *standing*, even the assessment of the ***LF*** component is inaccurate. For that reason, the ***LF*** and ***HF*** values were not used as single features in this work.

Because the cardiovascular system only needs one or two minutes to adapt to the new posture, a long term measurement is not useful. Therefore, time-domain methods might suit better for the evaluation of the orthostatic reaction. But additionally to the lowered orthostatic reaction, patients suffering from a neurodegenerative disease, have a considerably lower ***HRV*** in general

(***Parkinson's*** patient as example: see Figure 3.4). To include the information of a long term frequency based analysis, a possible approach would be the combination of time and frequency-based methods to extend the short-time evaluation with a long-time assessment of the ***ANS*** functionality with frequency-based***HRV*** measures.

Chapter 8

Conclusion and Outlook

The research goal of this work was to assess if it is possible to develop a system suited for ***HRV*** analysis in a home monitoring environment. For that purpose, the problem was separated into two tasks: The detection of posture changes during daily life activities which is supposed to trigger an ***HRV*** analysis or assessing an orthostatic reaction.

The main focus was the development of an algorithm which is able to detect common postures and postural changes in daily life. After optimization, the achieved recognition rate of detected postures was 92.93 %, whereas 81.14 % of the posture changes were detected correctly. Due to the huge amount of posture changes per day, the achieved recognition rate is sufficient for an accurate ***HRV*** analysis.

Furthermore, the developed algorithm should be capable of detecting and rejecting posture change events that are not suited for ***HRV*** analysis, such as events that occurred within a certain time period after a detected posture change or stand up events followed by physically high demanding activities, such as running or stair climbing. Because the system should be capable for home monitoring, the study design should simulate daily life activities. In order to further evaluate the robustness of the algorithm, future work should conduct a study with longer periods of keeping one posture and different types of activities with varying physical demands.

As the second part of this thesis, different time- and frequency-domain measures for ***HRV*** analysis were implemented and evaluated. Therefore, data was acquired before and after a posture change with a duration of 60 s each. In order to evaluate the orthostatic reaction the change of ***HRV*** measures during the stand-up event was computed. Results show a clear change in all computed measures.

Due to the long recording time, frequency based measures might not be as suitable for the evaluation of an orthostatic reaction, compared to time-domain methods. However, future work

could combine time-domain with frequency-based methods as additional input for the evaluation of the ***ANS*** functionality through long-term measurements

Because the proposed system is intended to be used for home monitoring it should be as unobtrusive as possible. Hence, an interesting approach would be using smartwatches measuring ***ECG*** (like the lastest version of the Apple Watch) instead of a regular ***ECG*** sensor with adhesive gel electrodes. However, this would require active participation of subjects since they need to touch the watch in order to close the electrical circuit.

This work shows a lot of improvements compared to the clinical Tilt Table Test procedure. Firstly, effects induced by the „*white coat syndrome*“ are lowered to a minimum because data is acquired in a home monitoring scenario and no medical staff who might induce further stress are present. Moreover, a larger number of posture change events, combined with ***HRV*** data, is available for further analysis.

Until now, the ***HRV*** analysis and the posture change detection were evaluated separately. As next step, future work should combine both algorithms and evaluate the performance in a long term study. In addition to that, it would be beneficial to extend the study by including subjects that are suffering from a orthostatic dysregulation. This would enable a better evaluation of the computed features for differentiating healthy subjects from patients with disorders of the ***ANS***.

Appendix A

Patents

A.1 Posture sensor automatic calibration

Publication Number	US20090312973A1
Date of Publication	Jun. 12,2008
Inventors	John D. Hatlestad Aaron Lewicke
Assignee	Cardiac Pacemakers Inc
Abstract	A system and method automatically calibrate a posture sensor, such as by detecting a walking state or a posture change. For example, a three-axis accelerometer can be used to detect a patient's activity or posture. This information can be used to automatically calibrate subsequent posture or acceleration data.

A.2 Posture and body movement measuring system

Publication Number	US7210240B2
Date of Publication	Feb. 23,2001
Inventors	Christopher P. Townsend, Steven W. Arms
Assignee	MicroStrain Inc
Abstract	A sensing device is attached to a living subject that includes a first sensors for distinguishing lying, sitting, and standing positions. In another embodiment, sensor data is stored in a storage device as a function of time. Multiple points or multiple intervals of the time dependent data are used to direct a feedback mechanism to provide information or instruction in response to the time dependent output indicating too little activity, too much time with a joint not being moved beyond a specified range of motion, too many motions beyond a specified range of motion, or repetitive activity that can cause repetitive stress injury.

A.3 System for detecting changes in body posture

Publication Number	US5865760A
Date of Publication	Nov. 25,1996
Inventors	Johan Lidman, Jonas Andersson
Assignee	Pacesetter AB
Abstract	In a system for detecting changes in body posture, electrocardiograms are recorded. The recorded electrocardiograms analyzed are to determine changes in the body posture of a patient from changes in the morphology of the recorded electrocardiograms. The electrocardiogram analysis can be augmented by obtaining and analyzing an accelerometer signal as well.

A.4 Multi-location posture sensing

Publication Number	US20080281381A1
Date of Publication	May. 07,2007
Inventors	Martin T. Gerber, John C. Rondoni
Assignee	Medtronic Inc
Abstract	Techniques for controlling therapy delivery based on the relative orientation and/or motion of a device accelerometer and a lead accelerometer are described. In one embodiment, a therapy system includes an electrical stimulator and a lead. The electrical stimulator comprises a processor that controls delivery of a therapy to a target stimulation site in a patient and a device accelerometer coupled to the electrical stimulator. The lead is coupled to the electrical stimulator to deliver the therapy from the electrical stimulator to the target stimulation site in the patient, and includes a lead accelerometer. The processor compares signals from the accelerometers, and controls delivery of the therapy to the patient based on the comparison. In this manner, the processor may adjust stimulation to, for example, address movement of electrodes relative to target tissue when a patient changes postures.

A.5 Physiological response to posture change

Publication Number	US20080082001A1
Date of Publication	Aug. 24,2006
Inventors	John D. Hatlestad, Imad Libbus, Aaron Lewicke
Assignee	Cardiac Pacemakers Inc
Abstract	In an embodiment, an implantable medical device includes a controller circuit, a posture sensing circuit, and a physiological sensing circuit. The controller circuit senses a change in a physiological signal as a result of a change in posture, and generates a response as a function of that change. In another embodiment, the controller circuit identifies a heart failure condition as a function of the change in the physiological signal.

A.6 Fitness score assessment based on heart rate variability analysis during orthostatic intervention

Publication Number	US20120108916A1
Date of Publication	Oct. 31,2010
Inventor	Alexander Riftine
Assignee	Alexander Riftine
Abstract	This invention relates to fitness monitors and the like. This invention is more particularly directed to a device and a method for facilitating quantitative evaluation of level of physical fitness (fitness score) including a PC or handheld, or watch type electronic device having input and output means based on formulas for calculating level of physical fitness through heart rate variability analysis during orthostatic intervention by assessing two main parameters, such as level of adaptation reserve and wellness level.

A.7 Method for quantitative assessment of the autonomic nervous system based on heart rate variability analysis

Publication Number US20090005696A1

Date of Publication Jun. 29,2007

Inventor Alexander Riftine

Assignee IntelWave LLC

Abstract A method is provided for characterizing autonomic nervous system activity of a patient based on heart rate variability analysis using electrocardiographic data from the patient. In addition, a computer-readable medium is provided tangibly embodying a program of instructions executable by a computer to perform a method for characterizing autonomic nervous system activity of a patient based on heart rate variability analysis using electrocardiographic data from the patient. Also, a system is provided for characterizing autonomic nervous system activity of a patient comprising a processor and a machine-readable medium tangibly embodying a program of instructions executable by the processor.

A.8 Method and apparatus for monitoring the autonomic nervous system using non-stationary spectral analysis of heart rate and respiratory activity

Publication Number US7079888B2

Date of Publication Apr. 11,2002

Inventors Harry Oung, Joseph Colombo

Assignee ANSAR GROUP Inc Ansar Inc

Abstract A method and apparatus for non-invasive, real-time monitoring of the autonomic nervous systems using non-stationary spectral analysis of both heart rate and respiratory signals. Continuous wavelet transformation is used in real-time so that the dynamic interactions between the sympathetic and parasympathetic divisions of the autonomic nervous system can be independently monitored in the frequency domain. The method in accordance with the present invention allows spectral analysis, formerly limited to the study of stationary data, to be applied to time-varying biological data such as heart rate variability and respiratory activity. In addition, the same techniques are used to monitor other biological or physiological data, including blood pressure.

Appendix B

Utilized chairs

Figure B.1: Utilized chairs for the posture change detection study with and without armrests

Glossary

ANS Autonomic Nervous System.

ECG Electrocardiogram.

FFT Fast Fourier Transformation.

HF high frequency.

HRV Heart Rate Variability.

IMU Inertial measurement unit.

LF low frequency.

PCA Principal Component Analysis.

Parkinson's Parkinson's Disease.

ULF ultra low frequency.

VLF very low frequency.

List of Figures

List of Tables

Bibliography

[Ale07] A. Aleksandrowicz, S. Leonhardt: *Wireless and Non-contact ECG Measurement System – the " Aachen SmartChair "*, *Acta Polytechnica*, Vol. 47, Nr. 4, 2007, pp. 5–8.

[Asc05] M. Aschner, L. G. Costa: *Environmental factors in neurodevelopmental and neurodegenerative disorders*, Cambridge University Press, 2005.

[Bea15] M. F. Beal, A. E. Lang, A. C. Ludolph: *Neurodegenerative diseases: Neurobiology, pathogenesis and therapeutics*, Elsevier, 2015.

[Ben96] D. G. Benditt, D. W. Ferguson, B. P. Grubb, B. B. Lerman, F. P. Cc, R. Sutton, D. Med, M. J. Wolk, L. Z. Douglas, D. W. Ferguson: *Acc expert consensus document Tilt Table Testing for Assessing Syncope*, *JACC*, Vol. 28, Nr. I, 1996, pp. 263–275.

[Ber97] G. G. Berntson, J. Thomas Bigger, D. L. Eckberg, P. Grossman, P. G. Kaufmann, M. Malik, H. N. Nagaraja, S. W. Porges, J. P. Saul, P. H. Stone, M. W. Van Der Molen: *Heart rate variability: Origins methods, and interpretive caveats*, *Psychophysiology*, Vol. 34, Nr. 6, 1997, pp. 623–648.

[Bid07] N. Bidargaddi, L. Klingbeil, A. Sarela, J. Boyle, V. Cheung, C. Yelland, M. Karunanithi, L. Gray: *Wavelet based approach for posture transition estimation using a waist worn accelerometer*, *Annual International Conference of the IEEE Engineering in Medicine and Biology - Proceedings*, 2007, pp. 1884–1887.

[Cer17] M. Cervelatti, U. Sunde: *Demographic Change and Long-run Development*, *MIT Press*, 2017.

[dT] I. de Telecomunicacoes: *biosppy.signals*, `https://biosppy.readthedocs.io/en/stable/biosppy.signals.html#biosppy-signals-ecg`, Accessed: 2019-01-03.

[Edo11] Edoardo: *Sagittal Plane*, `https://commons.wikimedia.org/wiki/File:Anatomical_Sagittal_Plane-en.svg`, 2011, Accessed: 2019-01-03.

[Fav09] J. Favre, R. Aissaoui, B. M. Jolles, J. A. Guise, K. Aminian: *Functional calibration procedure for 3D knee joint angle descriptions using intertial sensors*, *Journal of Biomechanics*, Vol. 42, Nr. 14, 2009, pp. 2330–2335.

[Gar13] C. A. García, A. Otero, X. Vila, D. G. Márquez: *A new algorithm for wavelet-based heart rate variability analysis*, *Biomedical Signal Processing and Control*, Vol. 8, Nr. 6, 2013, pp. 542–550.

[God14] A. Godfrey, G. Barry, J. C. Mathers, L. Rochester: *A comparison of methods to detect postural transitions using a single tri-axial accelerometer*, *2014 36th Annual International Conference of the IEEE Engineering in Medicine and Biology Society, EMBC 2014*, 2014, pp. 6234–6237.

[Haa01] T. H. Haapaniemi, V. Pursiainen, J. T. Korpelainen, H. V. Huikuri, K. A. Sotaniemi: *Ambulatory ECG and analysis of heart rate variability in Parkinson ' s disease*, *J Neurol Neurosurq Psychiatry*, Vol. 70, 2001, pp. 305–310.

[Ham02] P. Hamilton: *Open source ECG analysis*, *Computers in Cardiology*, 2002, pp. 101–104.

[Jan02] G. Janssen, H. B. Bussmann, H. J. Stam: *Determinants of the Sit-to-Stand Movement : A Review*, *Physical Therapy*, Vol. 82, Nr. 9, 2002, pp. 866–879.

[Kal00] M. Kallio, T. Haapaniemi, J. Turkka, K. Suominen, U. Tolonen, K. Sotaniemi, V. P. Heikkilä, V. Myllylä: *Heart rate variability in patients with untreated Parkinson's disease*, *European journal of neurology : the official journal of the European Federation of Neurological Societies*, Vol. 7, Nr. 6, 2000, pp. 667–672.

[Kan07] M. Kangas, A. Konttila, I. Winblad, T. Jämsä: *Determination of simple thresholds for accelerometry-based parameters for fall detection*, *Annual International Conference of the IEEE Engineering in Medicine and Biology - Proceedings*, 2007, pp. 1367–1370.

[Kim05] K. K. Kim, Y. K. Lim, K. S. Park: *Common Mode Noise Cancellation for Electrically Non-Contact ECG Measurement System on a Chair*, *2005 IEEE Engineering in Medicine and Biology 27th Annual Conference*, 2005, pp. 5881–5883.

[Kob09] H. Kobayashi: *Does Paced Breathing Improve the Reproducibility of Heart Rate Variability Measurements?*, *Journal of physiological anthropology*, Vol. 28, Nr. 5, 2009, pp. 225–230.

[Kud07] G. Kudaiberdieva, B. Görenek, B. Timuralp: *Heart rate variability as a predictor of sudden cardiac death*, *Anatolian journal of cardiology*, Vol. 7, Nr. suppl 1, 2007, pp. 68–70.

[Lan07] F. Lang, P. Lang: *Basiswissen Physiologie*, Springer, 2007.

[Lc01] M. Lamarre-cliche, J. Cusson: *The fainting patient: value of the head-upright tilt-table test in adult patients with orthostatic intolerance*, *CMAJ JAMC*, Vol. 164, Nr. 3, 2001, pp. 372–376.

[Lim06] Y. G. Lim, K. K. Kim, K. S. Park: *ECG Measurement on a Chair Without Conductive Contact*, *IEEE Transactions on biomedical engineering*, Vol. 53, Nr. 5, 2006, pp. 956–959.

[Low14] S. A. Lowe, G. Olaighin: *Monitoring human health behaviour in one's living environment: A technological review*, *Medical Engineering & Physics*, Vol. 36, 2014, pp. 147–168.

[Mih06] E. Mihci, F. Kardelen, B. Dora, B. S. Orthostatic: *Orthostatic heart rate variability analysis in idiopathic Parkinson ' s disease*, *Acta Neurol Scand*, Vol. 113, 2006, pp. 288–293.

[Mye86] G. A. Myers, G. J. Martin, N. M. Magid, P. S. Barnett, J. W. Schaad, J. S. Weiss, M. Lesch, D. H. Singer: *Power Spectral Analysis of Heart Rate Varability in Sudden Cardiac Death: Comparison to Other Methods*, *IEEE Transactions on Biomedical Engineering*, Vol. BME-33, Nr. 12, 1986, pp. 1149–1156.

[Naj02] B. Najafi, K. Aminian, F. Loew, Y. Blanc, P. A. Robert: *Measurement of Stand–Sit and Sit–Stand Transitions Using a Miniature Gyroscope and Its Application in Fall Risk Evaluation in the Elderly*, *Qualitative Research*, Vol. 49, Nr. 8, 2002, pp. 1–9.

[Num18] NumPy developers: *Numpy*, `http://www.numpy.org`, 2018, Accessed: 2019-01-02.

[Ope13] OpenStax College: *Blood Flow Through the Heart*, `https://upload.wikimedia.org/wikipedia/commons/f/f2/2101_Blood_Flow_Through_the_Heart.jpg`, 2013, Accessed: 2019-01-29.

[Owe99] P. Owens, N. Atkins, E. O. Brien: *Diagnosis of White Coat Hypertension by Ambulatory Blood Pressure Monitoring*, *Curr Hypertens Rep.*, Vol. 86, 1999, pp. 267–272.

[Pal14] E. Palermo, S. Rossi, F. Marini, F. Patanè, P. Cappa: *Experimental evaluation of accuracy and repeatability of a novel body-to-sensor calibration procedure for inertial sensor-based gait analysis*, *Measurement*, Vol. 52, 2014, pp. 145–155.

[Per07] H. Persson, M. Ericson, T. Tomson: *Heart rate variability in patients with untreated epilepsy*, *Seizure*, Vol. 16, Nr. 6, 2007, pp. 504–508.

[Pol07] T. Pola, J. Vanhala: *Textile Electrodes in ECG Measurement*, *3rd International Conference on Intelligent Sensors, Sensor Networks and Information*, 2007, pp. 635–639.

[Ric15] R. Richer: *Novel Human Computer Interaction Principles for Cardiac Feedback Using Google Glass and Android Wear*, Master's thesis, Friedrich Alexander Universität Erlangen-Nürnberg, 2015.

[Ric16] R. Richer, B. H. Groh, P. Blank, E. Dorschky, C. Martindale, J. Klucken, B. M. Eskofier: *Unobtrusive Real-time Heart Rate Variability Analysis for the Detection of Orthostatic Dysregulation*, *13th International Conference on Wearable and Implantable Body Sensor Networks (BSN 2016)*, 2016, pp. 189–193.

[Ros13] H. D. Rosario, A. Page, A. Besa, A. Valera: *Propagation of soft tissue artifacts to the center of rotation : a model for the correction of functional calibration techniques*, *Journal of Biomechanics*, Vol. 46, 2013, pp. 2619 – 2625.

[Sch99] J. D. Schipke, M. Pelzer, G. Arnold: *Heart rate variability: Standards of measurement, physiological interpretation and clinical use*, *Journal of Clinical and Basic Cardiology*, Vol. 2, Nr. 1, 1999, pp. 92–95.

[Wel67] P. D. Welch: *The Use of Fast Fourier Transform for the Estimation of Power Spectra: A Method Based on Time Averaging Over Short, Modified Periodograms*, *IEEE Transactions on audio and electroacoustics*, Vol. 2, 1967, pp. 70–73.

[Wie09] W. Wieling, I. J. Schatz: *The consensus statement on the definition of orthostatic hypotension: A revisit after 13 years*, *Journal of Hypertension*, Vol. 27, Nr. 5, 2009, pp. 935–938.

[Wil10] L. J. Williams: *Principal component analysis*, *Wires computional statistics*, 2010, pp. 433–459.

[Win83] B. B. Winter: *Driven-Right-Leg Circuit Design*, *IEEE Transactions on Biomedical Engineering*, Vol. BME-30, Nr. 1, 1983, pp. 62–66.

[Win05] R. Winker, W. Prager, A. Haider, B. Salameh, H. W. Rüdiger: *Schellong test in orthostatic dysregulation: A comparison with tilt-table testing*, *Wiener Klinische Wochenschrift*, Vol. 117, Nr. 1-2, 2005, pp. 36–41.

[Wor] WorldPress.com: *The ECG Leads, Polarity and Einthoven's Triangle*, `https://thephysiologist.org/study-materials/the-ecg-leads-polarity-and-einthovens-triangle/`, Accessed: 2019-01-15.

[Zij12] A. Zijlstra, M. Mancini, U. Lindemann, L. Chiari, W. Zijlstra: *Sit-stand and stand-sit transitions in older adults and patients with Parkinson ' s disease : event detection based on motion sensors versus force plates*, *Journal of neuroengineering and rehabilitation*, 2012, pp. 1–10.